

Makespan Trade-offs for Visiting Triangle Edges ^{★ ★★}

Konstantinos Georgiou, Somnath Kundu, and Paweł Prałat

Department of Mathematics, Toronto Metropolitan University, Toronto, Ontario, M5B 2K3,
Canada {konstantinos, somnath.kundu, pralat}@torontomu.ca

Abstract. We study a primitive vehicle routing-type problem in which a fleet of n unit speed robots start from a point within a non-obtuse triangle Δ , where $n \in \{1, 2, 3\}$. The goal is to design robots' trajectories so as to visit all edges of the triangle with the smallest visitation time makespan. We begin our study by introducing a framework for subdividing Δ into regions with respect to the type of optimal trajectory that each point P admits, pertaining to the order that edges are visited and to how the cost of the minimum makespan $R_n(P)$ is determined, for $n \in \{1, 2, 3\}$. These subdivisions are the starting points for our main result, which is to study makespan trade-offs with respect to the size of the fleet. In particular, we define $\mathcal{R}_{n,m}(\Delta) = \max_{P \in \Delta} R_n(P) / R_m(P)$, and we prove that, over all non-obtuse triangles Δ : (i) $\mathcal{R}_{1,3}(\Delta)$ ranges from $\sqrt{10}$ to 4, (ii) $\mathcal{R}_{2,3}(\Delta)$ ranges from $\sqrt{2}$ to 2, and (iii) $\mathcal{R}_{1,2}(\Delta)$ ranges from $5/2$ to 3. In every case, we pinpoint the starting points within every triangle Δ that maximize $\mathcal{R}_{n,m}(\Delta)$, as well as we identify the triangles that determine all $\inf_{\Delta} \mathcal{R}_{n,m}(\Delta)$ and $\sup_{\Delta} \mathcal{R}_{n,m}(\Delta)$ over the set of non-obtuse triangles.

Keywords: 2-Dimensional Search and Navigation · Vehicle Routing · Triangle · Make-span · Trade-offs.

1 Introduction

Vehicle routing problems form a decades old paradigm of combinatorial optimization questions. In the simplest form, the input is a fleet of robots (vehicles) with some starting locations, together with stationary targets that need to be visited (served). Feasible solutions are robots' trajectories that eventually visit every target, while the objective is to minimize either the total length of traversed trajectories or the time that the last target is visited.

Vehicle routing problems are typically NP-hard in the number of targets. The case of 1 robot in a discrete topology corresponds to the celebrated Traveling Salesman Problem whose variations are treated in numerous papers and books. Similarly, numerous vehicle routing-type problems have been proposed and studied, varying with respect to the number of robots, the domain's topology and the solutions' specs, among others.

[★] Research supported in part by NSERC.

^{★★} This is full version of the paper with the same title which will appear in the proceedings of the 32nd International Workshop on Combinatorial Algorithms (IWOC'A'21), 5-7 July 2021, Ottawa, Canada.

We deviate from all previous approaches and we focus on efficiency trade-offs, with respect to the fleet size, of a seemingly simple geometric variation of a vehicle routing-type problem in which targets are the edges of a non-obtuse triangle. The optimization problem of visiting all these three targets (edges), with either 1, 2 or 3 robots, is computationally degenerate. Indeed, even in the most interesting case of 1 robot, an optimal solution for a given starting point can be found by comparing a small number of candidate optimal trajectories (that can be efficiently constructed geometrically). From a combinatorial geometric perspective, however, the question of characterizing the points of an arbitrary non-obtuse triangle with respect to optimal trajectories they admit when served by 1 or 2 robots, e.g. the order that targets are visited, is far from trivial (and in fact it is still eluding us in its generality).

In the same direction, we ask a more general question: Given an arbitrary non-obtuse triangle, what is the worst-case trade-off ratio of the cost of serving its edges with different number of robots, over all starting points? Moreover, what is the smallest and what is the largest such value as we range over all non-obtuse triangles? Our main contributions pertain to the development of a technical geometric framework that allows us to pinpoint exactly the best-case and worst-case non-obtuse triangles, along with the worst-case starting points that are responsible for the extreme values of these trade-off ratios. To the best of our knowledge, the study of efficiency trade-offs with respect to fleet sizes is novel, at least for vehicle routing type problems or even in the realm of combinatorial geometry.

1.1 Motivation & Related Work

The main motivation for our work stems from its classification as a vehicle routing-type problem, first introduced by Dantzig and Ramser in 1959 [6]. In vehicle routing problems (VRPs), the primary objective is to minimize either the visitation time (makespan) or the total distance traveled to serve a set of targets using a fleet of (usually capacitated) robots. Early results on this topic are detailed in surveys such as [11,14].

While VRPs are typically studied in discrete domains, geometric vehicle routing problems have also been extensively explored, as seen in [7]. The long list of VRP variations proposed over time has led to numerous subject-focused surveys; see [10,12,13] for three relatively recent examples.

Famously, VRPs generalize the celebrated Traveling Salesman Problem (TSP), where a single vehicle must efficiently tour a set of targets. Similar to VRPs, TSP has numerous variations, including geometric ones [2,9], where targets are lines in the latter work. The natural extension of TSP to multiple vehicles is known as the Multiple Traveling Salesman Problem (MTSP) [5], a variant of VRPs where vehicles are uncapacitated. MTSP has also been studied with variations in the initial deployment of vehicles, either from a single location (single depot), as in our problem, or from multiple locations.

Apart from being related to vehicle routing problems, the geometric traveling salesman problem, and search and exploration games, our problem also relates to the so-called shoreline search problem, first introduced in [4]. Our research question arose from attempting to derive new lower bounds for this problem.

In the shoreline search problem, a unit robot searches for a hidden line on the plane, unlike our problem where the triangle edges are visible. The objective is to visit the line as quickly as possible relative to the distance from the robot's initial placement. The best known algorithm for this problem has a performance ratio of roughly 13.81, with only very weak (unconditional) lower bounds known [3]. Recently, the problem of searching with multiple robots was revisited, resulting in new lower bounds [1,8].

In typical online problems, a lower bound argument involves allowing an arbitrary algorithm to run for a certain time until the hidden item is placed at a location that the robot has not yet visited. The lower bound is then obtained by adding the elapsed time to the distance from the robot to the hidden item (the line), as it is assumed that the online algorithm has full knowledge of the input at this point. Applying this strategy to the shoreline problem involves identifying a number of lines as close as possible to the robot's starting point and computing the shortest trajectory for the robot to visit all of them, which mirrors our problem. This reasoning also applies to the case of multiple agents.

In the simplest configuration that could yield strong bounds, three lines forming a non-obtuse triangle are identified. The question then arises: what is the shortest trajectory that allows one (or multiple) agent(s) to visit all these edges? This question led to the research we present in this work. The motivation for restricting our attention to non-obtuse triangles is twofold: firstly, to address this specific configuration that arose from our motivating search problem, and secondly, because the optimal visitation cost for three robots in non-obtuse triangles is defined as the maximum distance over all triangle edges, treated as lines. Although our quantified results do not have immediate implications for the shoreline problem (or its lower bounds), we hope that the techniques we developed to compare optimal visitation trajectories by one or more agents will provide new insights for improving the lower bounds of the shoreline problem.

1.2 A Note on our Contributions & Paper Organization

We introduce and study a novel concept of efficiency/fleet size trade-offs in a special geometric vehicle routing-type problem that we believe is interesting in its own right. Deviating from the standard combinatorial perspective of the problem, we focus on the seemingly simple case of visiting the three edges of a non-obtuse triangle with $n \in \{1, 2, 3\}$ robots. Interestingly, the problem of characterizing the starting points within arbitrary non-obtuse triangles with respect to structural properties of the optimal trajectories they admit is a challenging question. More specifically, one would expect that the latter characterization is a prerequisite in order to analyze efficiency trade-offs when serving with different number of robots, over all triangles. Contrary to this intuition, and without fully characterizing the starting points of arbitrary triangles, we develop a framework that allows us (a) to pinpoint the starting points of any triangle at which these (worst-case) trade-offs attain their maximum values, and (b) to identify the extreme cases of non-obtuse triangles that set the boundaries of the inf and sup values of these worst-case trade-offs.

In Section 2.1 we give a formal definition of our problem, as well as we quantify our main results. Section 2.2 introduces some basic terminology, together with some preliminary and important observations. Then, in Section 3.1, we address first the basic question of visiting optimally two triangle edges, and we move in Section 3.2 to the problem of visiting optimally three triangle edges in a specific order. Section 4 is the beginning of our technical contribution, where we introduce a framework for characterizing triangle points with respect to optimal solutions they admit when serving with $n = 3, 2, 1$ robots, see Sections 4.1, 4.2 and 4.3, respectively. Using that framework, we expand our technical contribution by computing in Section 5 the visitation cost with 1, 2 robots of some special triangle starting points. Finally, in Section 6 we quantify the efficiency trade-offs with respect to the fleet size where, in particular, Sections 6.1, 6.2 and 6.3 focus on the cases of serving with 1 vs. 3 robots, 2 vs. 3 robots, and 1 vs. 2 robots, respectively.

2 Our Results & Basic Terminology and Observations

2.1 Problem Definition & Main Contributions

We consider the family of non-obtuse triangles \mathcal{D} , equipped with the Euclidean distance. For any $n \in \{1, 2, 3\}$, any given triangle $\Delta \in \mathcal{D}$, and any point P in the triangle, denoted by $P \in \Delta$, we consider a fleet of n unit speed robots starting at point P . A feasible solution to the triangle Δ visitation problem with n robots starting from P is given by robots' trajectories that eventually visit every edge of Δ , that is, each edge needs to be touched by at least one robot in any of its points including the end-points. The visitation cost of a feasible solution is defined as the makespan of robots' trajectory lengths, or equivalently as the first time by which every edge is touched by some robot. By $R_n(\Delta, P)$ we denote the optimal visitation cost of n robots, starting from some point $P \in \Delta$. When the triangle Δ is clear from the context, we abbreviate $R_n(\Delta, P)$ simply by $R_n(P)$.

In this work we are interested in determining visitation cost trade-offs with respect to different fleet sizes. In particular, for some triangle $\Delta \in \mathcal{D}$ (which is a compact set as a subset of \mathbb{R}^2), and for $1 \leq n < m \leq 3$, we define

$$\mathcal{R}_{n,m}(\Delta) := \max_{P \in \Delta} \frac{R_n(\Delta, P)}{R_m(\Delta, P)}.$$

Our main technical results pertain to the study of $\mathcal{R}_{n,m}(\Delta)$ as Δ ranges over all non-obtuse triangles \mathcal{D} . In particular, we determine $\inf_{\Delta \in \mathcal{D}} \mathcal{R}_{n,m}(\Delta)$ and $\sup_{\Delta \in \mathcal{D}} \mathcal{R}_{n,m}(\Delta)$ for all pairs $(n, m) \in \{(1, 3), (2, 3), (1, 2)\}$. Our contributions are summarized in Table 1.¹

For establishing the claims above, we observe that $\inf_{\Delta \in \mathcal{D}} \max_{P \in \Delta} \frac{R_n(\Delta, P)}{R_m(\Delta, P)} = \alpha$ is equivalent to that

$$\forall \Delta \in \mathcal{D}, \exists P \in \Delta, \frac{R_n(\Delta, P)}{R_m(\Delta, P)} \geq \alpha \quad \text{and} \quad \forall \epsilon > 0, \exists \Delta \in \mathcal{D}, \forall P \in \Delta, \frac{R_n(\Delta, P)}{R_m(\Delta, P)} \leq \alpha + \epsilon.$$

¹ Note that the entries in column 1 are not obtained by multiplying the entries of columns 2,3. This is because the triangles that realize the inf and sup values are not the same in each column.

	$\mathcal{R}_{1,3}(\Delta)$	$\mathcal{R}_{2,3}(\Delta)$	$\mathcal{R}_{1,2}(\Delta)$
$\inf_{\Delta \in \mathcal{D}}$	$\sqrt{10}$	$\sqrt{2}$	2.5
$\sup_{\Delta \in \mathcal{D}}$	4	2	3

Table 1: Our main contributions.

Similarly, $\sup_{\Delta \in \mathcal{D}} \max_{P \in \Delta} \frac{R_n(\Delta, P)}{R_m(\Delta, P)} = \beta$ is equivalent to that

$$\forall \Delta \in \mathcal{D}, \forall P \in \Delta, \frac{R_n(\Delta, P)}{R_m(\Delta, P)} \leq \beta \quad \text{and} \quad \forall \epsilon > 0, \exists \Delta \in \mathcal{D}, \exists P \in \Delta, \frac{R_n(\Delta, P)}{R_m(\Delta, P)} \geq \beta - \epsilon.$$

Therefore, as a byproduct of our analysis, we also determine the best and the worst triangle cases of ratios $\mathcal{R}_{n,m}(\Delta)$, as well as the starting points that determine these ratios. In particular we show that (i) the extreme values of $\mathcal{R}_{1,3}(\Delta)$ are attained as Δ ranges between “thin” isosceles and equilateral triangles, and the worst starting point is the incenter, (ii) the extreme values of $\mathcal{R}_{2,3}(\Delta)$ are attained as Δ ranges between right isosceles and equilateral triangles, and the worst starting point is again the incenter, and (iii) the extreme values of $\mathcal{R}_{1,2}(\Delta)$ are attained as Δ ranges between equilateral and right isosceles triangles, and the worst starting point is the middle of the shortest altitude.

2.2 Basic Terminology & Some Useful Observations

The length of segment AB is denoted by $\|AB\|$. An arbitrary non-obtuse triangle will be usually denoted by $\triangle ABC$, which we assume is of bounded size. More specifically, without loss of generality, we often consider $\triangle ABC$ represented in the Cartesian plane in *standard analytic form*, with $A = (p, q), B = (0, 0)$ and $C = (1, 0)$ (certain conditions imposed on p, q for the triangle to be non-obtuse and for AC to be the largest edge will be invoked when necessary). The following will be used repeatedly.

Observation 1 For $\triangle ABC$ in standard analytic form, where $A = (p, q)$, we have that

$$p = \frac{\cos(B) \sin(C)}{\sin(B+C)}, \quad q = \frac{\sin(B) \sin(C)}{\sin(B+C)}. \quad (1)$$

Therefore, for the incenter $I = (p_I, q_I)$ (the intersection of angle bisectors), we have

$$p_I = \frac{\cos(B/2) \sin(C/2)}{\sin((B+C)/2)}, \quad q_I = \frac{\sin(B/2) \sin(C/2)}{\sin((B+C)/2)}. \quad (2)$$

Proof. Consider the projection D of A onto BC . We have that $\tan(B) = \|AD\| / \|BD\|$, as well as $\tan(C) = \|AD\| / \|CD\|$. Therefore

$$\begin{aligned} \|BC\| &= \|BD\| + \|CD\| \\ &= \|AD\| \left(\frac{1}{\tan(B)} + \frac{1}{\tan(C)} \right) \\ &= \|AD\| \frac{\sin(C) \cos(B) + \cos(B) \sin(C)}{\sin(B) \sin(C)} \\ &= \|AD\| \frac{\sin(B+C)}{\sin(B) \sin(C)}. \end{aligned}$$

Since $\|BC\| = 1$, it follows that

$$q = \|AD\| = \frac{\sin(B) \sin(C)}{\sin(B+C)}.$$

Finally, we have

$$p = \|BD\| = \frac{\|AD\|}{\tan(B)} = \frac{\cos(B) \sin(C)}{\sin(B+C)},$$

and so (1) follows. Note that (2) is obtained as an immediate corollary, since $\triangle IBC$ is in analytic form too. \square

The next corollary is obtained after elementary algebraic manipulations.

Corollary 1. For $\triangle ABC$ in standard analytic form, its incenter $I = (p_I, q_I)$ is given by the formula

$$p_I = \frac{1}{2} \left(\sqrt{p^2 + q^2} - \sqrt{(p-1)^2 + q^2 + 1} \right), \quad q_I = \frac{q}{\sqrt{p^2 + q^2} + \sqrt{(p-1)^2 + q^2 + 1}}.$$

The cost of optimally visiting a collection of line segments \mathcal{C} (triangle edges) with 1 robot starting from point P is denoted by $d(P, \mathcal{C})$. For example, when $\mathcal{C} = \{AB, BC\}$ we write $d(P, \{AB, BC\})$. When, for example, $\mathcal{C} = \{AB\}$ is a singleton set, we slightly abuse the notation and for simplicity write $d(P, AB)$ instead of $d(P, \{AB\})$. Note that if the projection P' of P onto the line defined by points A, B lies in segment AB , then $d(P, AB) = \|PP'\|$, and otherwise $d(P, AB) = \min\{\|PA\|, \|PB\|\}$. The following observation follows immediately from the definitions, and the fact that we restrict our study to non-obtuse triangles.

Observation 2 For any non-obtuse triangle $\Delta = \triangle ABC$, and $P \in \Delta$, we have

- (i) $R_3(\Delta, P) = \max\{d(P, AB), d(P, BC), d(P, CA)\}$.
- (ii) $R_2(\Delta, P) = \min \left\{ \begin{array}{l} \max\{d(P, AB), d(P, \{BC, CA\})\} \\ \max\{d(P, BC), d(P, \{AB, CA\})\} \\ \max\{d(P, CA), d(P, \{BC, AB\})\} \end{array} \right\}$
- (iii) $R_1(\Delta, P) = d(P, \{AB, BC, CA\})$.

Motivated by our last observation, we also introduce notation for the cost of *ordered visitations*. Starting from point P , we may need to visit an *ordered list* of (2 or 3) line segments in a specific order. For example, we write $d(P, [AB, BC, AC])$ for the optimal cost of visiting the list of segments $[AB, BC, AC]$, in this order, with 1 robot. As we will be mainly concerned with $\triangle ABC$ edge visitations, and due to the already introduced standard analytic form, we refer to the trajectory realizing $d(P, [AB, BC, AC])$ as the (optimal) *LDR strategy* (L for “Left” edge AB , D for “Down” edge BC , and R for “Right” edge AC). We introduce analogous terminology for the remaining 5 permutations of the edges, i.e. LRD, RLD, RDL, DRL, DLR. Note that it may happen that in an optimal ordered visitation, robot visits a vertex of the triangle edges. In such a case we interpret the visitation order of the incident edges arbitrarily. For ordered visitation of 2 edges, we introduce similar terminology pertaining to (optimal) LD, LR, RL, RD, DR and DL strategies.

In order to obtain the results reported in Table 1, it is necessary to subdivide any triangle Δ into sets of points that admit the same optimal ordered visitations (e.g. all points P in which an optimal $R_1(\Delta, P)$ strategy is LRD). For $n \in \{2, 3\}$ robots, the subdivision is also with respect to the cost $R_n(\Delta, P)$. Specifically for $n = 2$, the subdivision is also with respect to whether the cost $R_2(\Delta, P)$ is determined by the robot that is visiting one or two edges (see Observation 2). We will refer to these subdivisions as the R_1, R_2, R_3 *regions*. For each $n \in \{1, 2, 3\}$, the R_n regions will be determined by collection (loci) of points between neighbouring regions that admit more than one optimal ordered visitations.

Angles are read counter-clockwise, so that for example for $\triangle ABC$ in standard analytic form, we have $\angle A = \angle BAC$. For aesthetic reasons, we may abuse notation and drop symbol \angle from angles when we write trigonometric functions. Visitation trajectories will be denoted by a list of points $\langle A_1, \dots, A_n \rangle$ ($n \geq 2$), indicating a movement along line segments between consecutive points. Hence, the cost of such trajectory would be $\sum_{i=2}^n \|A_i A_{i-1}\|$.

3 Preliminary Results

3.1 Optimal Visitations of Two Triangle Edges

We consider the simpler problem of visiting two distinguished edges of a triangle $\Delta = ABC$, starting from a point within the triangle. The following preliminary observations will be useful, and the reader may refer to Figures 1 and 2. Consider some $P \in \Delta$, and let K be on BC such that AK is the angle bisector of A . Any point on AK is equidistant from AB, AC . Moreover, for any $P \in ABK$ visiting AB is not more costly than visiting AC .

Now we consider the problem of visiting AB, AC starting from $P \in \Delta$. Let C', B' be the reflections of C, B around AB, AC , respectively. Clearly,

$$d(P, \{AB, AC\}) = \min\{d(P, AC'), d(P, AB')\}. \quad (3)$$

Since, in particular, AK is also the angle bisector of $C'AB'$, we conclude that if $P \in ABK$, then $d(P, \{AB, AC\})$ is determined by visiting AB no later than AC , that is, $d(P, \{AB, AC\}) = d(P, [AB, AC])$. In the remaining of this section, we fix such a P .

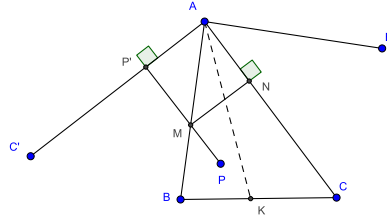


Fig. 1: Optimal trajectory for visiting $\{AB, AC\}$ for $\angle A \leq \pi/3$.

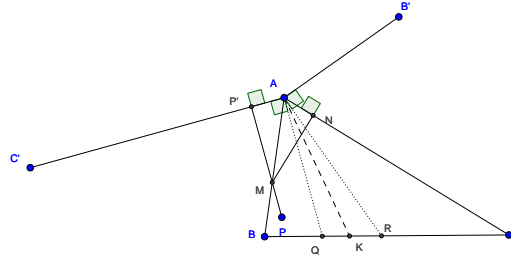


Fig. 2: Optimal trajectory for visiting $\{AB, AC\}$ for $\angle A \geq \pi/3$, starting outside the optimal bouncing subcone.

For the specifics of the optimal trajectory, we need some additional terminology. When $\angle A \geq \pi/3$, we define the concept of its *optimal bouncing subcone*, which is defined as a cone of angle $3\angle A - \pi$ and tip A , so that $\angle A$ and the subcone have the same angle bisector. When $\angle A = \pi/3$, then the optimal bouncing subcone is a ray with tip A that coincides with the angle bisector of $\angle A$. Whenever $\angle A < \pi/3$ we define its optimal bouncing subcone as the degenerate empty cone.

Observation 3 *If P is in the optimal bouncing subcone of $\angle A$, then $d(P, \{AB, AC\}) = \|PA\|$.*

Proof. Consider a line passing through A that is perpendicular to AC' that intersects BC at Q (see Figure 2). Consider also a line passing through A that is perpendicular to AB' that intersects BC at R . Then, the cone with tip A and angle $\angle QAR$ is the optimal bouncing subcone of $\angle A$. Let P be a point within the subcone. By construction, the projection of P onto the line defined by points A, C' falls outside the line segment AC' , and similarly for points A, B' . Therefore, for any point P within the subcone, we have that $d(P, AB') = d(P, AC') = \|PA\|$, so combined with (3), the claim follows. \square

For a point $P \in \triangle ABC$ outside the optimal bouncing subcone of $\angle A$, we define the (two) *optimal bouncing points* M, N of the ordered $[AB, AC]$ visitation as follows. Let P' be the projection of P onto AC' . Then, M is the intersection of PP' with AB and N is the projection of M onto AC . Note that equivalently, M, N are determined uniquely by requiring that (i) $\angle BMP = \angle NMA$, and (ii) $\angle ANM = \pi/2$.

Observation 4 *If P is outside the optimal bouncing subcone of $\angle A$, then $d(P, \{AB, AC\}) = \|PM\| + \|MN\|$, where M, N are the optimal bouncing points of ordered $[AB, AC]$ visitation.*

Proof. Since P in $\triangle ABK$, we have that $d(P, \{AB, AC\}) = d(P, [AB, AC])$. Also by (3), we have that $d(P, [AB, AC]) = \|PP'\|$. The claim follows by noticing that $\|MP'\| = \|MN\|$. \square

3.2 Optimal (Ordered) Visitation of Three Triangle Edges

In this section we discuss optimal LRD visitations of non-obtuse $\triangle ABC$, together with optimality conditions (recall that optimality refers to the cost incurred by one robot visiting all edges). Optimality conditions for the remaining 5 ordered visitations are obtained similarly. In order to determine the optimal LRD visitation, we obtain reflection C' of C across AB , and reflection B' of B across $C'A$, see also Figure 3.

From C' and A , we draw a lines ϵ, ζ , both perpendicular to $C'B'$ which may (or may not) intersect $\triangle ABC$. We refer to line ϵ as the *LRD bounce indicator line*. We also refer to line ζ as the *LRD subopt indicator line*. Each of the lines identify a halfspace on the plane. The halfspace associated with ϵ on the side of vertex A will be called the *positive halfspace of the LRD bounce indicator line* or in short the *positive LRD bounce halfspace*, and its complement will be called the *negative LRD bounce halfspace*. The halfspace associated with ζ on the side of vertex B will be called the *positive halfspace of the LRD subopt indicator line*, or in short the *positive LRD subopt halfspace*, and its complement will be called the *negative LRD subopt halfspace*.

For a point P in the positive LRD bounce and subopt halfspaces, let P' be its projection onto $C'B'$. Let E, F be the intersections of PP' with AB, AC' , respectively. Let also H be the reflection of F across AB , and let G be the projection of H onto BC . Points E, H, G will be called the *optimal LRD bouncing points* for point P . The points are also uniquely determined by requiring that $\angle BEP = \angle HEA$ and that HG is perpendicular to BC . For a point R in the negative LRD bounce halfspace and in the positive subopt halfspace, let J be the intersection of RC' with AB . Point J will be called the *degenerate optimal LRD bouncing point*, which is also uniquely determined by the similar bouncing rule $\angle BJR = \angle CJA$. Finally, let A', A'' be the projection of A onto $B'C', BC$, respectively.

The next lemma refers to such points P, R together with the construction of Figure 3. Its proof follows immediately by noticing that the optimal LRD visitation is in 1-1 correspondence with the optimal visitation of segment $B'C'$ using a trajectory that passes from segment AB .

Lemma 1. *The optimal LRD visitation trajectory, with starting points P, R, T , is:*

- trajectory $\langle P, E, H, G \rangle$, provided that P is in the positive LRD bounce and subopt halfspaces,
- trajectory $\langle R, J, C \rangle$, provided that R is in the negative LRD bounce halfspace and in the positive subopt halfspace,
- trajectory $\langle T, A, A'' \rangle$, provided that T is in the negative LRD subopt halfspace (see Figure 3).

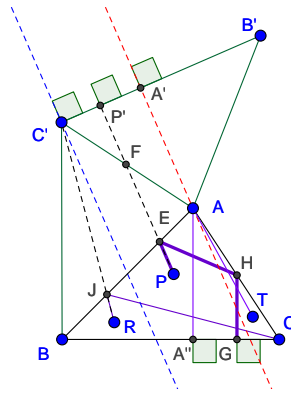


Fig. 3: Arbitrary non-obtuse $\triangle ABC$ shown with its LRD bounce indicator line (blue dotted line) and its LRD subopt indicator line (red dotted line).

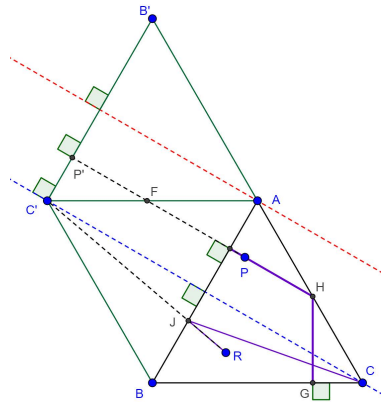


Fig. 4: Equilateral $\triangle ABC$ shown with its LRD bounce indicator line (blue dotted line) and its LRD subopt indicator line (red dotted line).

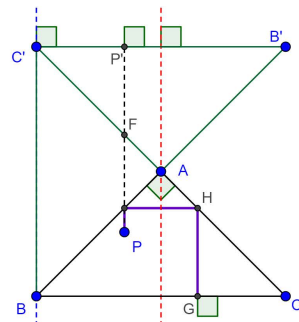


Fig. 5: Right isosceles $\triangle ABC$ shown with its LRD bounce indicator line (blue dotted line) and its LRD subopt indicator line (red dotted line).

4 Computing the R_n Regions, $n = 1, 2, 3$

By Observations 3, 4 and Lemma 1, we see that optimal visitations of 2 or 3 edges have cost equal to (i) the distance of the starting point to a line (reflection of some triangle edge), or (ii) the distance of the starting point to some point (triangle vertex) or (iii) the distance of the starting point to some triangle vertex plus the length of some triangle altitude. In this section we describe the R_n regions of certain triangles, $n \in \{1, 2, 3\}$. For this, we compare optimal ordered strategies, and the subdivisions of the regions are determined by loci of points that induce ordered trajectories of the same cost. As these costs are of type (i), (ii), or (iii) above (and considering all their combinations) the loci of points in which two ordered strategies have the same cost will be either some line (line bisector or angle bisector), or some conic section (parabola or hyperbola).

4.1 Triangle Visitation with 3 Robots - The R_3 Regions

Consider $\Delta \in \mathcal{D}$ with vertices A, B, C . For every $P \in \Delta$, any trajectories require time at least the maximum distance of P from all edges, in order to visit all of them. This bound is achieved by having all robots moving along the projection of P onto the 3 edges, and so we have $R_3(P) = \max\{d(P, AB), d(P, BC), d(P, CA)\}$, as also in Observation 2. Next we show how to subdivide the region of Δ with respect to which of the 3 projections is responsible for the optimal visitation cost. For this, we let I denote the incenter (the intersection of angle bisectors) of Δ . Let also K, L, M be the intersections of the bisectors with edges BC, CA and AB , respectively, see also Figure 6.

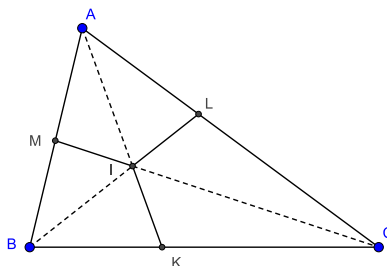


Fig. 6: The R_3 regions of an arbitrary non-obtuse ΔABC . AK, BL, CM are the angle bisectors of $\angle A, \angle B, \angle C$, respectively. Recall that the incenter I is equidistant from all triangle edges.

Lemma 2. *For every starting point $P \in \Delta$, we have that*

$$R_3(\Delta, P) = \begin{cases} d(P, AB) , & \text{provided that } P \in CLIK \\ d(P, BC) , & \text{provided that } P \in AMIL \\ d(P, CA) , & \text{provided that } P \in BKIM \end{cases} .$$

Proof. The subdivision of the R_3 regions are determined by the regions' separators, i.e. as per loci of points that are equidistant from the most distant edge. Since also the angle bisector is the locus of points that are equidistant from the lines forming the angle, the lemma follows. \square

4.2 Triangle Visitation with 2 Robots - The R_2 Regions

In this section we show how to subdivide the region of any non-obtuse triangle $\Delta \in \mathcal{D}$ into subregion with respect to the optimal trajectories and their costs, for a fleet consisting of 2 robots. The following lemma describes a geometric construction.

Lemma 3. Consider non-obtuse ΔABC along with its incenter I . Let K, M be the intersections of angle bisectors of A, C with segments BC, AB respectively. From K, M we consider cones of angles A, C respectively, having direction toward the interior of the triangle, and placed so that their bisectors are perpendicular to BC, AB , respectively. Then, the extreme rays of the cones intersect in line segment BI .

Proof. Consider non-obtuse triangle $\Delta = ABC$ and angle A bisector AK , where $K \in BC$. Let A' be the reflection of A across BC . Without loss of generality we may assume that $\angle B \geq \angle C$ or, in other words, that $\angle AKB \leq \pi/2$. First we consider the case that $\angle B > \angle C$, see Figure 7, and in particular that ΔABC is not isosceles (the case of isosceles triangle is much easier and can be treated similarly). Then

$$\angle A'BA + \angle BAC = 2\angle B + \angle A > \angle C + \angle B + \angle A = \pi,$$

and therefore BA' and AC are not parallel. Moreover the extensions of these line segments (on the directions of B, A , respectively) meet at a point, call it D .

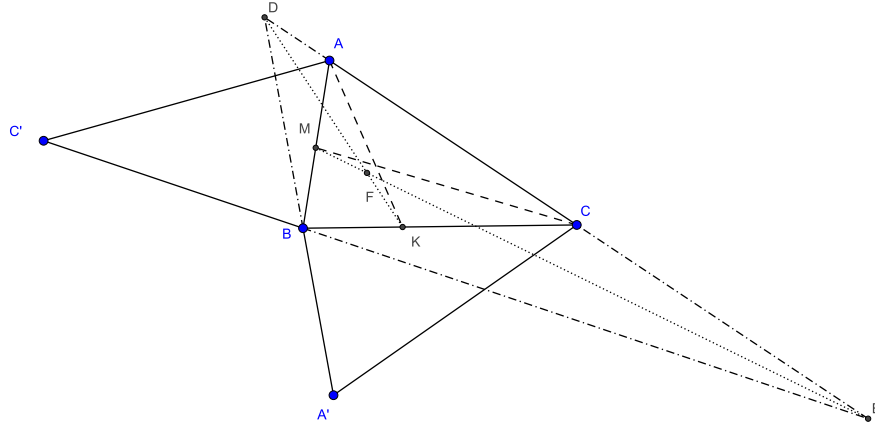


Fig. 7: The case of $\angle B > \angle C$, in the proof of Lemma 3.

Next we claim that DK is the angle bisector of $\angle A'DC$. To prove this, it suffices to show that K is the incenter of $\triangle DA'C$. Indeed, K lies on the bisector of $\angle ACA'$, since $\triangle A'BC$ was the result of the reflection of ABC across BC . For the same reason, K lies on the bisector of $\angle CA'B$ (which is an equivalent claim to that AK is the bisector of $\angle BAC$). Hence, K is the intersection of two bisectors of $\triangle DA'C$, as promised.

Next we denote by $\angle A, \angle B, \angle C$ the angles of $\triangle ABC$. We have the following claim: $\angle DKB = \pi/2 - \angle A/2$. Indeed,

$$\begin{aligned}
 \angle DKB &= \pi - \angle KBD - \angle BDK \\
 &= \pi - (\pi - \angle A'BC) - \angle A'DC/2 \\
 &= \angle B - (\pi - \angle CA'B - \angle DCA')/2 \\
 &= \angle B - \pi/2 + \angle A/2 + \angle C \\
 &= \pi - \angle A - \pi/2 + \angle A/2 \\
 &= \pi/2 - \angle A/2.
 \end{aligned}$$

In particular, this shows that KD is an extreme ray of a cone with tip K and angle $\angle A$, having direction toward the interior of the triangle, and placed so that its bisector is perpendicular to BC .

Similarly, consider the reflection of C across AB . Since $\angle A \neq \angle C$, the lines passing through pairs C', B and A, C are not parallel. So their extensions meet at some point, call it E , in the directions of points B, C respectively. Let also CM be the angle bisector of $\angle C$, where $M \in AB$. Exactly as before, EM is the angle bisector of $\angle AEB$, and hence all points on EM are equidistant from EA and EB . It follows that EM and DK intersect at the incenter of $\triangle BED$, call it F .

The above argument proves that F is the intersection of two of the extreme rays of the two cones with tips K, M and angles A, C , as per the description of the lemma. It remains to prove that F lies on the bisector of angle B . Indeed, F is on the bisector of $\angle DEB$ and on the bisector of $\angle EDB$. Therefore, F is the incenter of $\triangle BDE$. In particular, F should lie on the bisector of $\angle DBE$. Note however that $\angle DBE$ and $\angle ABC$ have the same bisector, because $\angle CBE = \angle ABD = \pi - 2\angle B$. \square

Motivated by Lemma 3, we will be referring to the subject point F in the line segment BI as the *separator of the angle B bisector*. Similarly, we obtain separators J, H of angles C, A bisectors, respectively, see also Figure 8.

In what follows, we will be referring to the (possibly non-convex) hexagon $MFKJLH$ as the R_2 *hexagon separator* of $\triangle ABC$.

From the proof of Lemma 3 we also derive a useful observation. Referring to Figure 7, recall that DK is the angle bisector of $\angle A'DC$. Therefore all points on DK are equidistant from DA' and AC . At the same time the distance of any point P on FK to DA' equals $d(P, \{AB, BC\}) = d(P, [BC, AB])$ unless $d(P, \{AB, BC\}) = \|PB\|$, that is, unless the optimal strategy for visiting $\{AB, BC\}$ would be to move directly to vertex B (which happens only if $\angle B \geq \pi/3$ and P lies within the optimal bouncing subcone of angle B , see Observation 3).

The remaining of the section refers to non-obtuse triangle $\Delta = \triangle ABC$ as in Figure 8, where in particular $MFKJLH$ is the R_2 separator of Δ . We are now in a position to make a preliminary observation which will be generalized soon. Suppose that

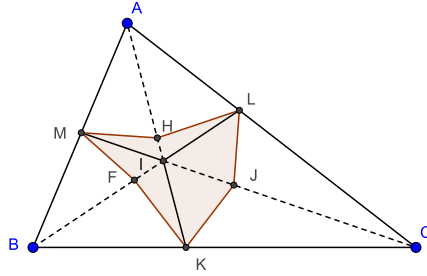


Fig. 8: The R_2 hexagon separator of $\triangle ABC$.

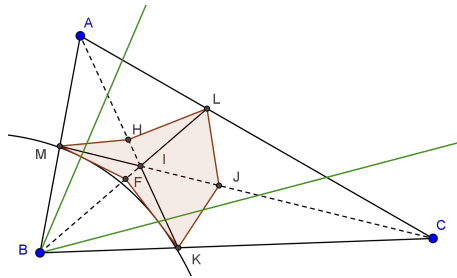


Fig. 9: The refined R_2 mixed-hexagon separator of $\triangle ABC$, where $\angle B > \pi/3$.

$\angle B \leq \pi/3$. Then for every point P either on MF or on FK , we have that $d(P, AC) = d(P, \{BC, AB\})$. Moreover, for every P within tetragon $BKFM$, we have that $R_2(P) = d(P, AC)$.

The previous observation can be extended to larger angles. Assume that $\angle B \geq \pi/3$. Then, the same reasoning shows that for every point P either on MF or on FK , which are outside the optimal bouncing subcone of angle B , we have that $d(P, AC) = d(P, \{BC, AB\})$. For points within the subcone, the optimal trajectory to visit $\{BC, AB\}$ would be to go directly to B . So for points P within the optimal bouncing subcone, condition $d(P, AC) = d(P, \{BC, AB\})$ translates into that P is equidistant from AC and B . Hence, P lies in a parabola with AC being the directrix and B being the focus. Next, we refer to that parabola as the *separating parabola of B*.

Motivated by the previous observation, we introduce the notion of the *refined R_2 mixed-hexagon separator of triangle Δ* as follows. For every angle of Δ which is more than $\pi/3$, we replace the portion of the R_2 hexagon separator within the optimal bouncing subcone of the same angle by the corresponding separating parabola. In Figure 9 we display an example where only one angle is more than $\pi/3$. Combined with Observation 2 (ii), we can formalize our findings as follows.

Lemma 4. *For every starting point on the boundary of the refined R_2 mixed-hexagon separator of a triangle Δ , the cost of visiting only the opposite edge equals the cost of visiting the other two edges. For every starting point P outside the R_2 separator, $R_2(P)$ equals the distance of P to the opposite edge. Moreover, for every starting point P in*

the interior of the refined R_2 separator, $R_2(P)$ is determined by the cost of visiting two of the edges of Δ .

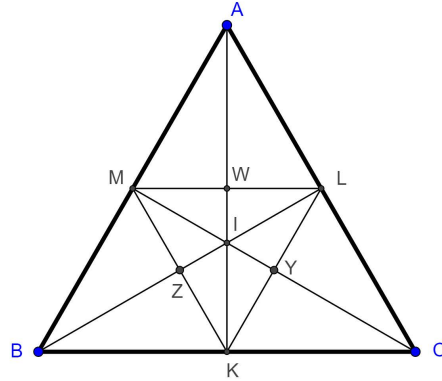


Fig. 10: The R_2 regions of the equilateral triangle, see also Corollary 2 and Corollary 4 for detailed description.

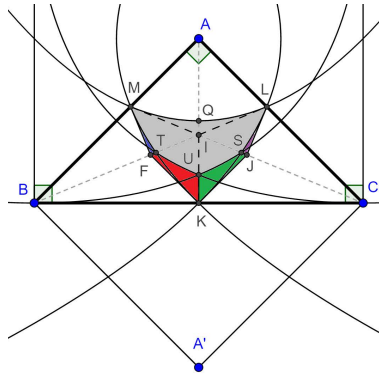


Fig. 11: The R_2 regions of the right isosceles, see also Corollary 3 and Lemma 5 for detailed description. The coloured region identifies the refined R_2 mixed-hexagon separator.

Lemma 4 implies the following corollaries pertaining to specific triangles ΔABC . In both statements, and the associated figures, I is the incenter of the triangles, and points K, L, M are defined as in Figure 6.

Corollary 2 (Hexagon separator of equilateral triangle). Consider equilateral $\Delta = \Delta ABC$, see Figure 10. Let W, Z, Y be the intersections of AK, BL, CM respectively (also the separators of angle A bisector, angle B bisector, and angle C bisector, respectively). Then, the R_2 hexagon separator of Δ is $MZKYLW$, which is also triangle MKL . More specifically, for all $P \in \Delta AML$, we have that $R_2(\Delta, P) = d(P, BC)$.

By symmetry, one can derive $R_2(\Delta, P)$ for all starting points P outside the hexagon separator of isosceles Δ .

Corollary 3 (Mixed-hexagon separator of right isosceles). *Consider right isosceles $\Delta = \triangle ABC$, see Figure 11. The separator of angle A bisector is incenter I . Let also F, J be the separators of angle B bisector and angle C bisector, respectively. Then, the R_2 hexagon separator of Δ is $IMFKJL$. The parabola with directrix BC and focus A , intersecting AK at Q and passing through M, L is the separating parabola of A . Hence, for every point $P \in \Delta$ above the parabola, we have $R_2(\Delta, P) = d(P, BC)$, as well as for every point X in tetragon $MBKF$, we have $R_2(\Delta, X) = d(X, AC)$. The remaining case of starting points in tetragon $KCLJ$ follows by symmetry.*

Describing the subdivisions within the refined R_2 mixed-hexagon separator for arbitrary triangles is a challenging task. On the other hand, by Observation 2 (ii) and Lemma 4 the cost within the separator is determined by the cost of visiting just two edges. Also, by Observations 3, 4 the cost of such visitation can be described either as a distance to a line or to a point. We conclude that, within the R_2 separator, the subdivisions are determined by separators that are either parts of lines or parabolas (loci of points for which the cost of visiting some two edges are equal). Hence, for any fixed triangle, an extensive case analysis pertaining to pairwise comparisons of visitations costs can determine all R_2 subdivisions (and the challenging ones are within the refined separator). In what follows we summarize formally the subdivisions only of two triangle types, focusing on the visitation cost of all starting points within the (refined) hexagon separators.

Corollary 4 (R_2 regions of an equilateral triangle). *Consider equilateral $\Delta = \triangle ABC$, as in Corollary 2, see Figure 10. Then for every starting point $P \in \triangle MWI$, we have that $R_2(\Delta, P) = d(P, [AB, AC])$. The remaining cases of starting points within the hexagon separator $MZKYLW$ follow by symmetry.*

Lemma 5 (R_2 regions of a right isosceles triangle). *Consider right isosceles $\Delta = \triangle ABC$, as in Corollary 3, see Figure 11. Consider parabola with directrix the line passing through B that is perpendicular to BC (also the reflection of BC across AB) and focus A , passing through M, K and intersecting BL at point T (define also S as the symmetric point of T across AK). That parabola is the locus of points P for which $\|PA\| = d(P, [AB, BC])$. Let also A' be the reflection of A across BC . Consider parabola with directrix BA' and focus A , passing through T and intersecting AK at point U . That parabola is the locus of points P for which $\|PA\| = d(P, [BC, AB])$. Therefore, if P is a starting visitation point, we have that:*

- $R_2(\Delta, P) = \|PA\|$, for all P in mixed closed shape $MTUSLQ$ (grey shape in Figure 11),
- $R_2(\Delta, P) = d(P, [AB, BC])$, for all P in mixed closed shape MFT (blue shape in Figure 11),
- $R_2(\Delta, P) = d(P, [AC, BC])$, for all P in mixed closed shape LJS (purple shape in Figure 11),
- $R_2(\Delta, P) = d(P, [BC, AB])$, for all P in mixed closed shape $FKUT$ (red shape in Figure 11).
- $R_2(\Delta, P) = d(P, [BC, AC])$, for all P in mixed closed shape $JSUK$ (green shape in Figure 11).

Proof. For every starting point P within the refined R_2 mixed-hexagon separator, the cost $R_2(\Delta, P)$ is determined by the visitation cost of two edges.

Note that the optimal bouncing subcone of $\angle A$ is one with extreme rays AB, AC (i.e. the angle itself). Hence, by Observation 3, for every P in mixed closed shape $MTUSLQ$, we have that $d(P, \{AB, AC\}) = \|PA\|$. Therefore, by the definitions of the separating parabolas, we have that $R_2(\Delta, P) = \|PA\|$.

Consider now some starting point P in mixed closed shape MFT . By the definition of the separating parabolas, we have that

$$R_2(\Delta, P) = d(P, \{AB, BC\}) = d(P, [AB, BC]),$$

where the last equality follows since P is not below line segment BL , the angle bisector of $\angle B$ (and $d(P, [AB, BC])$ can be computed as the distance of P to the reflection of BC across AB).

Finally, consider some starting point P in mixed closed shape $FKUT$. By the definition of the separating parabolas, we have that

$$R_2(\Delta, P) = d(P, \{AB, BC\}) = d(P, [BC, AB]),$$

where the last equality follows since P is not above line segment BL , the angle bisector of $\angle B$. \square

4.3 Triangle Visitation with 1 Robot - The R_1 Regions

In this section we show how to partition the region of an arbitrary non-obtuse $\triangle ABC$ into sets of points P with respect to the optimal strategy of $R_1(P)$. There are 6 possible visitation strategies for $d(P, \{AB, AC, BC\})$, one for each permutation of the edges indicating the order they are visited (ordered visitations). Clearly, it is enough to describe, for each two ordered visitations, the borderline (separator) of points in which the two visitations have the same cost. By Lemma 1, any such ordered visitation cost is the distance of the starting point either to a point, or to a line, or a distance to a line plus the length of some altitude. Since the R_1 regions are determined by separators, i.e. loci of points in which different ordered visitations induce the same costs, it follows that these separators are either lines, or conic sections. Therefore, by exhaustively pairwise-comparing all ordered visitations along with their separators, we can determine the R_1 regions of any triangle. Next, we explicitly describe the R_1 regions only for three types of triangles that we will need for our main results. For the sake of avoiding redundancies, we omit any descriptions that are implied by symmetries.

The next lemma describes the R_1 regions of an equilateral triangle, as in Figure 12.

Lemma 6 (*R_1 regions of an equilateral triangle*). *Consider equilateral triangle $\triangle ABC$ with angle bisectors AK, BL, CM and incenter I . Then, the angle bisectors are the loci of points in which optimal ordered visitations have the same cost. Moreover, for every starting point $P \in \triangle AMI$, the optimal strategy of $R_1(\Delta, P)$ is LRD visitation.*

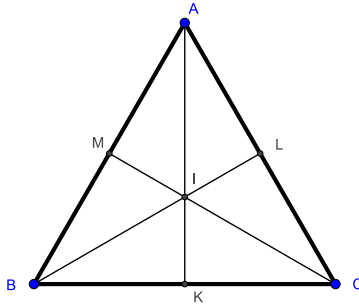


Fig. 12: The R_1 regions of an equilateral triangle.

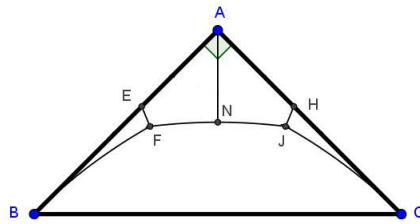


Fig. 13: The R_1 regions of a right isosceles triangle.

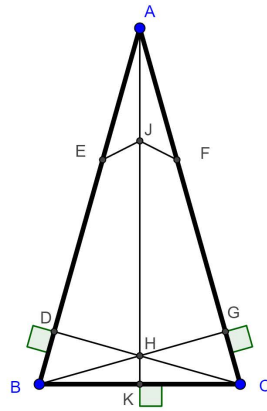


Fig. 14: The R_1 regions of an isosceles triangle ABC with small $\angle A$.

Proof. Points on AI are in the positive LRD and RDL bounce and subopt halfspaces, since AI is the bisector of $\angle A$. As such, points on segment AI are the loci of points P , for which

$$d(P, \{AB, BC, AC\}) = d(P, [AB, AC, BC]), d(P, [AC, AB, BC]),$$

i.e. the points in which the optimal R_1 visitation is both LRD and RLD. To see why, note that by Figure 4 we have that $d(P, [AB, AC, BC]) = \|PP'\|$. Considering the reflection of C'' of C' around A , and the reflection B'' of B around A , it is easy to see that the bisector of the line formed by $B'C'$ and $B''C''$ coincides with the altitude of $\triangle ABC$ corresponding to BC (this property is actually true for every non-obtuse triangle). Since $\triangle ABC$ is equilateral triangle, its altitude corresponding to BC is also the angle $\angle A$ bisector. \square

The next lemma describes the R_1 regions of a right isosceles, as in Figure 13. Curve FJ is part of the parabola with directrix the reflection of BC across A and focus the reflection of A across BC . Curve BF is part of the parabola with directrix a line parallel to AB which is $\|AB\|$ away from AB , and focus the reflection of A across BC . Curve CJ is part of the parabola with directrix a line parallel to AC which is $\|AC\|$ away from AC , and focus the reflection of A across BC . CE (not shown in the figure) is the bisector of $\angle C$, and segment EF is part of the reflection of that bisector across AB . BH is the bisector of $\angle C$, and segment HJ is part of the reflection of that bisector across AC . Segment AN is part of the altitude corresponding to A .

Lemma 7 (R_1 regions of a right isosceles triangle). *Consider right isosceles $\Delta = \triangle ABC$, and starting point P . Then, the optimal visitation strategy for $R_1(\Delta, P)$ is:*

- an LRD visitation, if $P \in AEFN$,
- an LDR visitation if $P \in BFE$, and
- both an DRL, DLR visitation if $P \in BCJF$ (trajectory visits $\{AB, AC\}$ at point A).

Proof. The reader may consult Figure 13. As in the proof of Lemma 6, points on AN are the loci of points in which the optimal strategy is both LRD and RLD. Points P in $AEFN$ are in the positive LRD bounce and subopt halfspace, and so by Lemma 1, $R_1(\Delta, P) = d(P, B'C')$, where B', C' are the reflections of B, C across A , respectively (points B', C' along with the LRD bounce indicator line and the LRD subopt indicator line are depicted separately in Figure 5). Points P in region $BCJF$ are in the negative DRL (and DLR) bounce halfspace and in the positive subopt halfspace, and so by Lemma 1, we have that $R_1(\Delta, P)$ is obtained by a degenerate bouncing trajectory visiting both AB, AC at point A . Considering the reflection A' of A across BC , the cost in this case would be $\|PA'\|$. Hence, the loci of points P for which $d(P, B'C') = \|PA'\|$ is the parabola described in the statement of the lemma, whose portion reads as curve FJ .

The rest of the separators follow using similar arguments. Indeed, line segment EF is the loci of points in which the optimal R_1 visitation is both LDR and LRD (so the separator is formed by the reflection of the angle bisector of the angle across the first visited edge, a property that can be shown for every non-obtuse triangle). Finally, the curve BF (part of a parabola, as described in the statement of the lemma), is the loci of points P for which the optimal R_1 visitation is LDR and has cost equal to $\|PA'\|$.

The analysis for the rest of the depicted separators is identical, due to the triangle's symmetry along the bisector of $\angle A$ (that coincides with AN). \square

Next we consider a “thin” isosceles $\Delta = \triangle ABC$ with $\angle A \leq \pi/3$, as in Figure 14. (Eventually we will invoke the next lemma for $\angle A \rightarrow 0$.) AK is the altitude corresponding to A . CD, BG are the altitudes corresponding to AB, AC , respectively. CE, BF (not shown) are the extreme rays of the optimal bouncing subcone corresponding to C, B , respectively. H is the intersection of AK with BG (and CD), i.e. the orthocenter of the triangle. Segment EJ (as part of a line) is the reflection of EC (as part of a line) across AB . Segment FJ (as part of a line) is the reflection of BF (as part of a line) across AC .

Lemma 8 (R_1 regions of a thin isosceles triangle). *Consider isosceles $\Delta = \triangle ABC$, with $\angle A \leq \pi/3$ and starting point P . Then, the optimal visitation strategy for $R_1(\Delta, P)$ is:*

- an LRD visitation if $P \in AEJ$,
- both LRD and LDR (optimal strategy is to visit first AB and then move to C), if $P \in EDHJ$,
- an LDR visitation, if $P \in DBH$, and
- a DLR visitation if $P \in BKH$.

Proof. The separator AK is justified as in the proof of Lemma 6. Points in region AEJ are in the positive LRD bounce and subopt halfspace, and so by Lemma 1, the optimal R_1 visitation is given as a distance of P to a line. Points in region $EDHJ$ are in the negative LRD bounce and positive subopt halfspace, and so by Lemma 1, the optimal R_1 visitation is given as a distance of P to a point (the projection C' of C across AB). The transition in which the optimal visitation does not visit vertex C happens exactly at segment EJ whose extension passes through C' , and in particular has the property that JC' is perpendicular to BC' . Finally, the justification of separator segments DH, BH is identical to the reasoning of the equilateral triangle (see Figure 12) as provided in the proof of Lemma 6. \square

5 Optimal Visitations of Some Special Starting Points

5.1 R_2 Cost of the Incenter

Lemma 9. *Consider $\triangle ABC \in \mathcal{D}$ with largest angle vertex C and incenter I . Then $R_2(I) = \|IC\|$.*

Proof. Incenter I is equidistant from all edges of $\triangle ABC$. Since in every optimal R_2 strategy, one robot visits an edge and the other visits the remaining two (which is at least as costly as visiting any one edge), the cost of $R_2(I)$ equals the cheapest cost of visiting any two edges of $\triangle ABC$. Now, since $\angle C$ is the largest angle, it follows that $\angle C \geq \pi/3$, and hence by Observation 3 we have that $d(I, \{AC, BC\}) = \|IC\|$. Therefore, the claim follows once we prove that $\|IC\| \leq \max\{d(I, \{AB, BC\}), d(I, \{BA, AC\})\}$, or equivalently once we prove that $\|IC\| \leq d(I, \{AB, BC\})$, for every $\angle B \leq \angle C$.

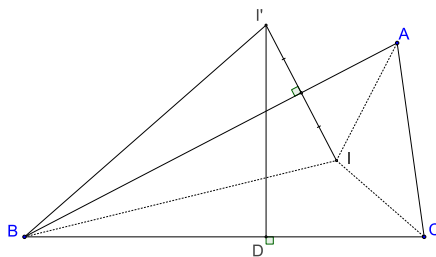


Fig. 15: Showing that $\|IC\| \leq \max\{d(I, \{AB, BC\}), d(I, \{BA, AC\})\}$.

Since $\angle C$ is the dominant angle, it follows that $\angle B \leq \pi/3$, see also Figure 15. Consider the reflection I' of I around AB , and the projection D of I' onto BC (because $\angle B \leq \pi/3$, point D falls within segment BC). Then, by Observation 4, we have $d(I, \{AB, BC\}) = \|I'D\|$. So it remains to prove that $\|IC\| \leq \|I'D\|$. For that we employ the standard analytic form of $\triangle ABC$. For notational convenience, we introduce notation $\alpha = \|BC\| = 1$, $\beta = \|AC\| = \sqrt{(1-p)^2 + q^2}$ and $\gamma = \|AB\| = \sqrt{p^2 + q^2}$.

Note that $\angle B \leq \pi/3$, and hence $\sqrt{3}/2 \geq \sin(B) = q/\gamma$. Moreover, since $\angle C \geq \pi/3$, we have $\sqrt{3}/2 \leq \sin C = q/\beta$. Combining the two inequalities we get the following condition

$$3(1-p)^2 \leq q^2 \leq 3p^2, \quad (4)$$

which in particular (combined with that $p \leq 1$) implies that $1/2 \leq p \leq 1$.

By Corollary 1, the coordinates of the incenter $I = (x, y)$ can be computed as

$$x = \frac{\gamma + p}{1 + \beta + \gamma}, \quad y = \frac{q}{1 + \beta + \gamma}.$$

Point $I' = (x', y')$ can be computed by rotating I by angle B (using the Cartesian system), so it follows that $\|I'D\| = y' = x \sin(B) + y \cos(B)$. After elementary algebraic manipulations, we obtain that

$$\|I'D\| - \|IC\| = \frac{1}{(1 + \beta + \gamma)^2} \left(\frac{4p^2q^2 + 4pq^2\sqrt{p^2 + q^2}}{p^2 + q^2} - (1 + \sqrt{(1-p)^2 + q^2} - p)^2 \right).$$

It is easy to see that $\frac{4p^2q^2 + 4pq^2\sqrt{p^2 + q^2}}{p^2 + q^2}$ is increasing in p , and that $(1 + \sqrt{(1-p)^2 + q^2} - p)^2$ is decreasing in p (when $p \in [0, 1]$). Hence, using also (4), a lower bound to $\|I'D\| - \|IC\|$ is obtained by setting $3(1-p)^2 = q^2$ or by setting $q^2 = 3p^2$ (and the valid lower bound would be the minimum of the two). Next we will use that $1/2 \leq p \leq 1$.

Elementary calculations show that when $3(1-p)^2 = q^2$, we have

$$\|I'D\| - \|IC\| \geq - \frac{3(p-1)^2 \left(2p \left(-2\sqrt{4p^2 - 6p + 3} + 4p - 9 \right) + 9 \right)}{4p^2 - 6p + 3}.$$

The real roots of the latter function of p are $p = 1/2, 1$. Hence, $\|I'D\| - \|IC\|$ preserves sign for all $p \in [1/2, 1]$, and the sign is the same as, say, when $p = 2/3$, in which case the value of the function becomes $\frac{9}{7} \left(\frac{8\sqrt{7}}{27} + \frac{16}{27} \right) - 1 \approx 0.76981 \geq 0$.

Finally, when $q^2 = 3p^2$, we obtain that

$$\|I'D\| - \|IC\| \geq 2p - \sqrt{4p^2 - 2p + 1}.$$

The latter continuous expression of p has only one real root $p = 1/2$, and it is clearly positive when $p \geq 1/2$. Hence, we conclude again that $\|I'D\| - \|IC\| \geq 0$, as wanted. \square

5.2 R_1 Cost of the Incenter

Lemma 10. *For non-obtuse $\triangle ABC$ with incenter I , let $\angle A$ be its largest angle. Then, $R_1(I) = \|IA'\|$, where A' is the reflection of A across BC .*

Proof. The reader may consult Figure 16. Point C' is the reflection of C across AB , and B' the reflection of B across AC' . First we observe that the optimal trajectory that visits first BC has cost $\|IA'\|$, that is, the optimal such strategy is both of DLR and DRL type. Indeed, it is easy to see that I is in the negative DLR bounce halfspace and in the positive subopt halfspace. Hence, by Section 3.2, the optimal such strategy is of degenerate bouncing type, where the bouncing point J on BC (intersection point of BC and IA') lies within the optimal bouncing subcone of angle A (and hence $d(J, \{AB, AC\}) = JA$), and the claim follows.

In order to prove that the DLR (and DRL) type strategy with cost

$$\|IA'\| = d(I, \{AB, BC, AC\})$$

is optimal, we will compare it with the optimal LRD type and the optimal LDR strategy (and the symmetric argument would also imply the same comparison with the optimal RLD and RDL strategies).

Comparison with optimal LRD strategy: Next we compare the optimal DLR strategy above with an optimal LRD strategy. There are three cases to consider.

Case (a): I lies in the positive LRD bounce halfspace and in the negative LRD subopt halfspaces (I lies within the optimal bouncing subcone of $\angle C'$, when necessarily $\angle C \geq \pi/3$), in which case the optimal LRD strategy has cost $\|IC'\|$, see Figure 18.

Case (b): I lies in the negative LRD subopt halfspace, hence, the optimal LRD strategy has cost $\|IA\| + h_A$, where h_A is the altitude corresponding to angle A , see Figure 17.

Case (c): I lies in the positive LRD bounce and subopt halfspaces and, in particular, the cost of the optimal LRD trajectory is $d(I, B'C')$ (depicted as $\|IN\|$ in Figure 16).

We have the following observation.

Observation 5 *I lies in the positive LRD bounce and subopt halfspaces exactly when $3A - 2C \leq \pi$ and*

$$\cos^2(C) \cos^2\left(\frac{B+C}{2}\right) \geq \frac{\sin^2\left(\frac{3A}{2}\right) \sin^2\left(\frac{C}{2}\right)}{-2\cos(B+C) + 2\cos(B) - 2\cos(C) + 3}$$

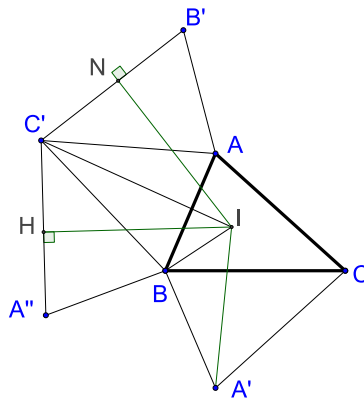


Fig. 16: Comparison between the optimal DRL strategy with the optimal LRD and optimal LDR strategies.

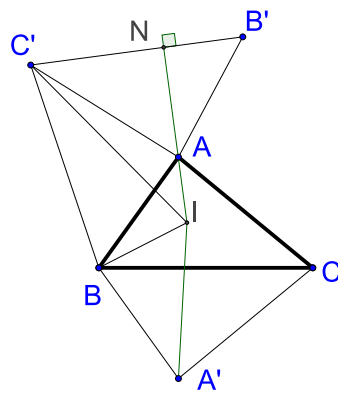


Fig. 17: The boundary case of Observation 5, where the optimal LRD strategy has cost $\|IA\| + h_A$.

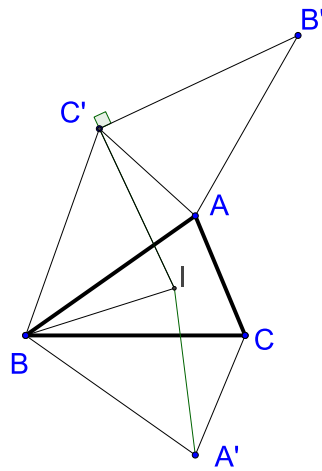


Fig. 18: The boundary case of Observation 5, where the optimal LRD strategy has cost $\|IC'\|$.

Proof. Let N denote the projection of I onto the line passing through C', B' . For I to lie in the positive LRD bounce and subopt halfspaces, we need that N falls within segment $B'C'$ and that IN intersects segment AB . When I, A, N become collinear (see Figure 17), it is easy to see that $A/2 + A + \pi/2 - C = \pi$, or equivalently that $3A - 2C = \pi$. It follows immediately that IN intersects AB in its interior only when $3A - 2C \leq \pi$. Similarly, let ρ denote $\angle AC'I$, see Figure 18. Point N coincides with C' exactly when $\rho + C = \pi/2$, and when $\rho + C \leq \pi/2$ point N lies within $B'C'$. Now, using the Sine Law in $\triangle C'IA$, we see that $\sin(\rho) = \frac{\|IA\|}{\|IC'\|} \sin(3A/2)$. Since $\rho + C \leq \pi/2$ is equivalent to that $\sin^2(\rho) \leq \sin^2(\pi/2 - C)$, our condition becomes

$$\cos^2(C) \geq \frac{\|IA\|^2}{\|IC'\|^2} \sin^2(3A/2).$$

The latter expression can be simplified (after trigonometric manipulations), using also (1) and (2) of Observation 1, together with that $C' = (\cos(2B), \sin(2B))$, resulting in the promised condition. \square

Case (a) proof: From Observation 1, we have that

$$\begin{aligned} \|IA'\|^2 &= (p_I - p)^2 + (q_I + q)^2 \\ &= 4 \sin^2\left(\frac{B}{2}\right) \sin^2\left(\frac{C}{2}\right) (2 \cos(B+C) + 2 \cos(B) + 2 \cos(C) + 3) \csc^2(B+C). \end{aligned} \quad (5)$$

Observe that point C' is also obtained by rotating point $C = (1, 0)$ by $2\angle B$, and hence $C' = (\cos(2B), \sin(2B))$. Therefore,

$$\begin{aligned} \|IC'\|^2 &= (\cos(2B) - p_I)^2 + (\sin(2B) - q_I)^2 \\ &= \sin^2\left(\frac{B}{2}\right) (-2 \cos(B+C) + 2 \cos(B) - 2 \cos(C) + 3) \csc^2\left(\frac{B+C}{2}\right). \end{aligned}$$

Let $f(B, C) := \|IC'\|^2 / \|IA'\|^2$, so that our goal is to show that $f(B, C) \geq 1$, subject to that $\angle A$ is the largest angle. We claim that $f(B, C)$ is decreasing in C . Indeed, elementary calculations show that

$$\frac{\partial}{\partial C} f(B, C) = - \frac{\cos\left(\frac{B}{2}\right) \csc^3\left(\frac{C}{2}\right) \cos\left(\frac{B+C}{2}\right)}{(2 \cos(B+C) + 2 \cos(B) + 2 \cos(C) + 3)^2} g(B, C),$$

where

$$\begin{aligned} g(B, C) &= 2 \cos(B-C) - 4 \cos(B+C) - 2 \cos(2B+C) + 2 \cos(B+2C) \\ &\quad + 4 \cos(B) + 2 \cos(2B) + 4 \cos(C) + 1. \end{aligned}$$

Note that $\frac{\partial}{\partial C} f(B, C)$ is a product of expressions (multiplied by -1), and clearly all of them, except possibly $g(B, C)$, are non-negative. Therefore, it remains to show that $g(B, C) \geq 0$. In order to do that we consider two sub-cases.

Sub-case i: If $B \leq \pi/4$, then the only summand of $g(B, C)$ which is negative is $2 \cos(B + 2C)$. Then, we have

$$\begin{aligned} g(B, C) &\geq 4 \cos(C) + 4 \cos(B) + 2 \cos(B + 2C) \\ &\geq 4 \cos(C) + 2 \cos(B) + 2 \cos(B + 2C) \\ &= 4 \cos(C) + 4 \cos(B + C) \cos(C) \\ &\geq 4 \cos(C) - 4 \cos(C) \\ &\geq 0, \end{aligned}$$

where the second to last inequality holds because $B + C \leq 2\pi/3$ (since A is the largest angle and hence $A \geq \pi/3$).

Sub-case ii: If $B > \pi/4$, then the only two summands of $g(B, C)$ which may be negative are $2 \cos(2B)$ and $2 \cos(B + 2C)$. Recalling that $A \geq \pi/3$, and using the monotonicity of the cosine function, we get the following sequence of inequalities:

$$\begin{aligned} 1 + 4 \cos(B) + 2 \cos(2B) &\geq -1 \\ 2 \cos(B - C) &\geq 2 \cos(\pi/12) = \frac{\sqrt{3} + 1}{\sqrt{2}} \\ 4 \cos(C) &\geq 4 \cos(5\pi/12) = \sqrt{2}(\sqrt{3} - 1) \\ -4 \cos(B + C) &\geq -4 \cos(\pi/2) \geq 0 \\ -2 \cos(2B + C) &\geq -2 \cos(3\pi/4) = \sqrt{2} \\ 2 \cos(B + 2C) &\geq -2. \end{aligned}$$

So, overall we have that

$$g(B, C) \geq 3\sqrt{\frac{3}{2}} + \frac{1}{\sqrt{2}} - 3 > 0,$$

as wanted. Hence, $f(B, C)$ is decreasing in C , as promised.

But then, since $A \geq C$, we have that $C \leq \pi/2 - B/2$, and hence it follows that

$$f(B, C) \geq f(B, \pi/2 - B/2) = 1,$$

where the last equality follows by direct substitution. That completes the proof of case (a).

Case (b) proof: Let N' be the projection of A onto BC , so that AN' is the altitude corresponding to angle A . We want to prove that $\|IA'\| \leq \|IA\| + \|AN'\|$. By triangle inequality, we have that $\|IA'\| \leq \|IN'\| + \|N'A'\| = \|IN'\| + \|AN'\|$. Hence, it suffices to prove that $\|IN'\| \leq \|IA\|$.

Using the standard analytic form of the triangle, we have that

$$\|IA\|^2 - \|IN'\|^2 = (q_I - q)^2 - q_I^2 = q(q - 2q_I).$$

Hence, it further suffices to prove that $q \geq 2q_I$. Indeed,

$$\frac{q}{q_I} = 2 \frac{\cos(\frac{B}{2}) \cos(\frac{C}{2})}{\cos(\frac{B+C}{2})} =: g(B, C)$$

We have that

$$\frac{\partial}{\partial C} g(B, C) = \frac{\sin(B)}{1 + \cos(B + C)} \geq 0.$$

Hence, $g(B, C) \geq g[B, 0] = 2$, where the last equality follows by direct substitution. That completes the proof of case (b).

Case (c) proof: The analytic equation of the line ℓ passing through B', C' has equation

$$\ell : \tan(2A)x + y - \sin(2B) - \tan(2A)\cos(2B) = 0. \quad (6)$$

To see why, recall that from the proof of case (a) above we have that

$$C' = (\cos(2B), \sin(2B)),$$

as well as ℓ form with the x -axis an angle of $\pi - 2A$. But then, using the formula for the distance of point $I = (p_I, q_I)$ to ℓ we have that

$$d(I, B'C') = \frac{|\tan(2A)p_I + q_I - \sin(2B) - \tan(2A)\cos(2B)|}{\sqrt{\tan^2(2A) + 1}}.$$

Using (2) of Observation 1, together with (5), and after trigonometric manipulations, it follows that

$$\left(\frac{d(I, B'C')}{\|IA'\|} \right)^2 = \frac{\cos^2\left(\frac{B+C}{2}\right)(-2\cos(B+2C) + 2\cos(C) + 1)^2}{2\cos(B+C) + 2\cos(B) + 2\cos(C) + 3}, \quad (7)$$

which we need to prove is at least 1. Call function (7) $h_1(B, C)$. Function $h_1(B, C)$ attains values as low as 9/10 without conditioning on that I lies the positive LRD bounce and subopt halfspaces.

Consider the domain $\mathcal{D}_1 \subseteq \mathbb{R}^2$ of (7) corresponding to non-obtuse $\triangle ABC$ with $\angle A \geq \angle B, \angle C$ and restricted to $3\angle A - 2\angle C \leq \pi$ (as per Observation 5).

Lemma 11. *Function $h_1(B, C)$ is concave over domain \mathcal{D} .*

Proof. We show that function (7) is concave by verifying numerically that it's Hessian $H_{B,C}$ is negative-definite. Matrix $H_{B,C}$ is a 2×2 symmetric real matrix, whose real roots can be computed analytically. The domain \mathcal{D}_1 can be re-parameterized as

$$0 \leq B \leq 3\pi/7, \quad \max\{\pi/2 - B, (2\pi - 3B)/5\} \leq C \leq \min\{2\pi/3 - B, \pi/2 - B/2, \pi - 2B\}$$

so that the eigenvalues can be plotted over \mathcal{D} as it is shown in Figure 19. \square

Now, by Lemma 11, any (local) minimizers of function (7) are attained at the boundaries of its domain. Subject to that any of the boundaries of Observation 5 are satisfied tightly, function $h_1(B, C)$ is at least 1, as already proven in cases (a), (b). The remaining constraints that might be tight are that $A \geq B, C$.

Subject to that $B = A$, we have that

$$h_1(B, \pi - 2B) = \frac{\sin^2\left(\frac{B}{2}\right)(2\cos(2B) + 2\cos(3B) - 1)^2}{3 - 2\cos(2B)}.$$

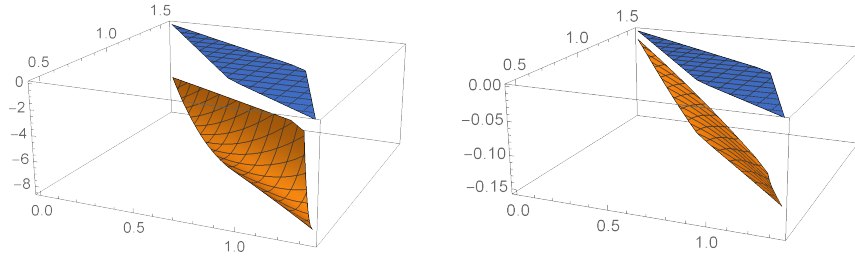


Fig. 19: The two eigenvalues of Hessian $H_{B,C}$ of function (7) are compared to blue hyperplane $z = 0$ over domain \mathcal{D}_1 .

The function above can be shown to be concave when $B \in [\pi/3, \pi/2]$, hence its minima are attained at the boundaries of its domain. When $B = \pi/3$ its value is 1. When $B = 3\pi/7$ its value is equal to

$$\frac{\sin^2\left(\frac{3\pi}{14}\right)\left(1 + 2\sin\left(\frac{3\pi}{14}\right) + 2\cos\left(\frac{\pi}{7}\right)\right)^2}{3 + 2\cos\left(\frac{\pi}{7}\right)} \approx 1.32715.$$

Finally, subject to that $C = A$, it is easy to see that the linear constraints imply that the smallest value that C can attain is $\pi/3$. At the same time, the nonlinear constraint of Observation 5 becomes (for $C = A$)

$$\frac{\cos^2(C)(3 - 2\cos(2C))\csc^4\left(\frac{C}{2}\right)}{(2\cos(C) + 1)^2} \geq 1.$$

It can be shown that the above constraint is satisfied only when $C \leq \pi/3$. It follows that when $A = C$, we must have $A = B = C = \pi/3$, in which case $h_1(\pi/3, \pi/3) = 1$.

Comparison with optimal LDR strategy: In order to describe the optimal LDR strategy, we also consider the reflection A'' of A across BC' , so that the cost of such strategy equals the distance of I to segment $C'A''$, see also Figure 16. Let also H denote the projection of I onto $C'A''$. As before, we have the following cases to consider. Case (a'): I lies the positive LDR bounce halfspace and in the negative LDR subopt halfspaces, in which case the optimal LDR strategy has cost $\|IC'\|$. Case (b'): I lies in the negative LDR subopt halfspace, hence, the optimal LDR strategy has cost $\|IB\| + h_B$, where h_B is the altitude corresponding to angle B . Case (c'): I lies the positive LDR bounce and subopt halfspaces, and in particular the cost of the optimal LDR trajectory is $d(I, C'A'')$ (depicted as $\|IH\|$ in Figure 16).

Observation 6 I lies in the positive LDR bounce and subopt halfspaces exactly when $3B - 2C \leq \pi$ and

$$\cos^2(2C)\cos^2\left(\frac{B+C}{2}\right) \leq \frac{\sin^2\left(\frac{3A}{2}\right)\sin^2\left(\frac{C}{2}\right)}{-2\cos(B+C) + 2\cos(B) - 2\cos(C) + 3}.$$

Proof. As in the proof of Observation 5, let ρ denote $\angle AC'I$. When I, B, H become collinear, it is easy to see that $B/2 + B + \pi/2 - C = \pi$, or equivalently that $3B - 2C = \pi$. It follows immediately that IH intersects BC' in its interior only when $3B - 2C < \pi$. Point H coincides with C' exactly when $C - \rho + C = \pi/2$, and when $2C - \rho + C \leq \pi/2$ point H lies within B', C' . Using $\sin(\rho)$ that was computed in the proof of Observation 5, we obtain condition

$$\cos^2(2C) \leq \frac{\|IA\|^2}{\|IC'\|^2} \sin^2(3A/2).$$

The latter expression can be simplified (after trigonometric manipulations), using also (1) and (2) of Observation 1, together with that $C' = (\cos(2B), \sin(2B))$, resulting in the promised condition. \square

Case (a') proof: This case is identical to case (a) above.

Case (b') proof: Let N' be the projection of A onto BC , so that AN' is the altitude h_A corresponding to angle A . By triangle inequality, we have that $\|IA'\| \leq \|IN'\| + h_A$. At the same time, the optimal LDR visitation in this case has cost $\|IB\| + h_B \geq h_A$, where the inequality is due to that $\angle A$ is the dominant angle, hence h_A is the shortest altitude. Hence, it suffices to argue that $\|IB\| \geq \|IN'\|$, which is immediate $\|IB\|^2 = p_I^2 + q_I^2$, while $\|IN'\|^2 = (p_I - p)^2 + q_I^2$.

Case (c') proof: The analytic equation of the line ℓ passing through C', A'' has equation

$$\ell: -\tan(2B - C)x + y - \sin(2B) + \tan(2B - C)\cos(2B) = 0.$$

To see why, recall that from the proof of case (c) above we have that

$$C' = (\cos(2B), \sin(2B)),$$

as well as ℓ forms with the x -axis an angle of $2B - C$. But then, using the formula for the distance of point $I = (p_I, q_I)$ to ℓ we have that

$$d(I, \ell) = \frac{|-\tan(2B - C)p_I + q_I - \sin(2B) + \tan(2B - C)\cos(2B)|}{\sqrt{\tan^2(2B - C) + 1}}.$$

Using (2) of Observation 1, together with (5), and after trigonometric manipulations, it follows that

$$\left(\frac{d(I, \ell)}{\|IA'\|}\right)^2 = \frac{(2\cos(B - C) + 2\cos(C) + 1)^2 \cos^2\left(\frac{B+C}{2}\right)}{2\cos(B + C) + 2\cos(B) + 2\cos(C) + 3}, \quad (8)$$

which we need to prove is at least 1. Call function (8) $h_2(B, C)$. As in the previous case, $h_2(B, C)$ can attain values below 1 without conditioning on that I lies in the positive LDR bounce and subopt halfspaces (in which case $d(I, C'A'') = d(I, \ell)$, as per Observation 6).

Recall that $\triangle ABC$ is non-obtuse with $\angle A \geq \max\{\angle B, \angle C\}$, and that $3\angle B - 2\angle C \leq \pi$ (as per Observation 6). The domain \mathcal{D}_2 defined by these linear constraints can be described as follows:

$$0 \leq B \leq 3\pi/7, \quad \max\{\pi/2 - B, (3B - \pi)/2\} \leq C \leq \min\{2\pi/3 - B, \pi/2 - B/2, \pi - 2B\}.$$

Unfortunately, $h_2(B, C)$ is not concave over \mathcal{D}_2 , however we can still show numerically that any minimizers are attained at the boundaries of the domain (and the boundary imposed by the non linear constraint of Observation 6).

Lemma 12. *Function $h_2(B, C)$ has no minimizers in the interior of domain \mathcal{D}_2 .*

Proof. We demonstrate, numerically, that the gradient of function $h_2(B, C)$ is never the zero vector over \mathcal{D}_2 . In fact, as Figure 20 shows, $\partial h_2(B, C)/\partial B$ does not attain value 0 in domain \mathcal{D}_2 .² \square

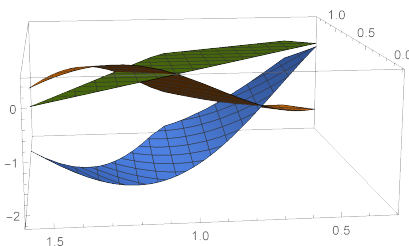


Fig. 20: The plot of $\partial h_2(B, C)/\partial B$ (blue) and $\partial h_2(B, C)/\partial C$ (orange) over domain \mathcal{D}_2 , compared with the hyperplane $z = 0$ (green plane).

Now, by Lemma 12, any (local) minimizers of $h_2(B, C)$ are attained at the boundaries of its domain. Subject to that, any of the boundaries of Observation 6 are satisfied tightly, function $h_2(B, C)$ is at least 1, as already proven in cases (a'), (b'). The remaining constraints that might be tight are that $\angle A \geq \max\{\angle B, \angle C\}$. Subject to that $B = A$, we have that $h_2(B, \pi - 2B) = h_1(B, \pi - 2B)$ which was shown to be at least 1 previously, subject to that $\pi/3 \leq (3\pi/7)B$ (the same bounds hold for B using the current linear conditions). Finally, subject to that $C = A$, it is easy to see, exactly as before, that the linear constraints imply that the smallest value that C can attain is $\pi/3$. At the same time, the nonlinear constraint of Observation 6 becomes (for $C = A$)

$$\frac{\sin^2\left(\frac{3C}{2}\right) \sec^2(2C)}{3 - 2 \cos(2C)} \geq 1.$$

It can be shown that the above constraint is satisfied only when $\pi/6 \leq C \leq \pi/3$. It follows that when $A = C$, we must have $A = B = C = \pi/3$, in which case $h_2(\pi/3, \pi/3) = 1$.

\square

² By considering a sufficiently refined grid, we can numerically (and rigorously) verify that the function is bounded away from 0, as seen in the figure. The claim then follows by theoretical bounds on the partial derivatives of the expression.

5.3 R_1 Cost of the Middle Point of the Shortest Altitude

Lemma 13. *For a non-obtuse $\triangle ABC$ with $\angle A \geq \angle B \geq \angle C$, let T be the middle point of the altitude corresponding to the largest edge BC . Then the optimal $R_1(T)$ strategy is of LRD type, and has cost $\frac{1}{2}(2 - \cos(2A)) \sin(B) \sin(C) \csc(B + C)$.*

Consider $\triangle ABC$ in standard analytic form, with altitude AF . Let C', B' be the reflection of C, B across AB, AC' , respectively (see also Figure 21). Since $\angle A \geq \angle B \geq \angle C$, it is easy to verify that T is always in the positive LRD bounce and subopt halfspaces. Hence, the projection G of T along $B'C'$ falls within the latter segment, and in particular by Lemma 1, the optimal LRD strategy has cost $d(T, B'C') = \|TG\|$. What we show is that $R_1(T) = \|TG\|$ by comparing $\|TG\|$ to the cost of the remaining optimal ordered visitations the triangle edges.

Comparison to optimal LDR strategy: Consider the reflection A' of A across BC' , and let H be the projection of T along $C'A'$, see Figure 21. Clearly the optimal LDR strategy has cost at least $d(T, C'A') = \|TH\|$. The loci of points P that are equidistant from $C'A', C'B'$ are exactly on the angle bisector of $\angle C'$. Moreover, there is no triangle configuration that T falls on the latter angle bisector. To see why, consider the bisector CM of $\angle C$ (hence $C'M$ is the bisector of $\angle C'$). Because $\angle A \geq \angle B \geq \angle C$, we have $\|BM\| \leq \|MA\|$, and hence CM intersects AF below T . That also shows that T remains always closer to the $B'C'$ segment.

Comparison to optimal DLR and DRL strategies: Consider the reflection A' of A across BC . Let also C'', B'' be the reflections of C, B across BA', CA' respectively, see also Figure 22. It is easy to see that, since $\angle A \geq \angle B \geq \angle C$, point T is always in the negative DLR (and DRL) bounce halfspace and in the positive subopt halfspace. It follows by Lemma 1 that both optimal DLR and DRL strategies have cost $\|TA'\| = \frac{3}{2}q$.

We compute $d(T, B'C') = \|TG\|$ using (6). Since $T = (p, q/2)$, it follows that

$$\begin{aligned} \|TG\| &= \frac{|\tan(2A)p + q/2 - \sin(2B) - \tan(2A) \cos(2B)|}{\sqrt{\tan^2(2A) + 1}} \\ &= \frac{1}{2}(2 - \cos(2A)) \sin(B) \sin(C) \csc(B + C). \end{aligned} \quad (9)$$

Now, using Observation 1 we have that

$$\frac{\|TG\|}{\|TA'\|} = \frac{1}{3}(2 - \cos(2A)) \leq 1,$$

as wanted.

Comparison to optimal RDL strategy: Consider the reflection B'', A' of B, A across AC and $B''C$, respectively, see Figure 23. Since $\angle A \geq \angle B \geq \angle C$, point T is always in the negative RDL bounce halfspace and in the positive subopt halfspace. It follows by Lemma 1 that the optimal RDL strategy has cost $\|TB''\|$.

Note that by shifting the origin by $(-1, 0)$, point B'' is obtained as the rotation of $(-1, 0)$ by angle $-2C$. Hence,

$$B'' = R_{-2C} \begin{pmatrix} -1 \\ 0 \end{pmatrix} + \begin{pmatrix} 1 \\ 0 \end{pmatrix} = \begin{pmatrix} 1 - \cos(2C) \\ \sin(2C) \end{pmatrix}.$$

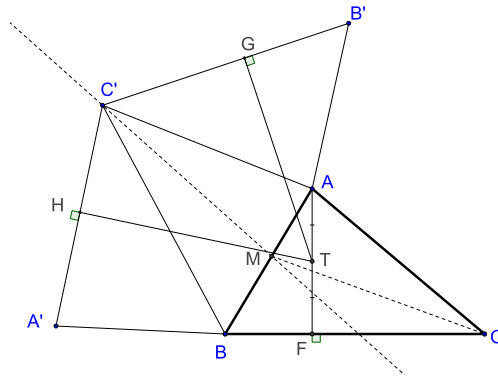


Fig. 21: Comparison of optimal LRD with optimal LDR strategy.

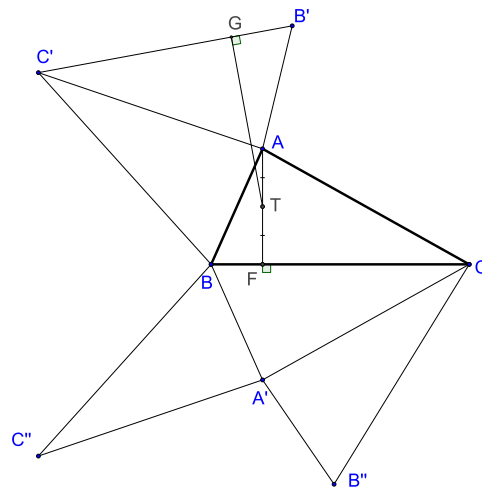


Fig. 22: Comparison of optimal LRD with optimal DLR and DRL strategies.

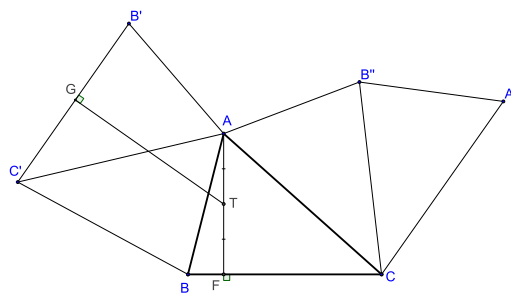


Fig. 23: Comparison of optimal LRD with optimal RDL strategy.

Therefore, the optimal RDL strategy has cost

$$\begin{aligned}\|TB''\| &= \sqrt{(1 - \cos(2C) - p)^2 + (\sin(2C) - q/2)^2} \\ &= \frac{1}{2\sqrt{2}} \frac{\sin(C)}{\sin(B+C)} \sqrt{-4\cos(2(B+C)) - \cos(2B) + 4\cos(2C) + 9}.\end{aligned}$$

It follows, after trigonometric manipulations, that

$$\frac{\|TB''\|^2}{\|TG\|^2} = \frac{(-4\cos(2(B+C)) - \cos(2B) + 4\cos(2C) + 9)}{2(\cos(2(B+C)) - 2)^2 \sin^2(B)}.$$

Call the latter function $f(B, C)$. We have that

$$\begin{aligned}\frac{\partial}{\partial C} f(B, C) &= \frac{10\sin(2(B+C)) - 2\sin(4(B+C)) - \sin(4B+2C) + 2\sin(2B+4C) + 6\sin(2B) + 7\sin(2C)}{(\cos(2(B+C)) - 2)^3}.\end{aligned}$$

Recall that $\angle A \geq \angle B \geq \angle C$. Since also the triangle is non-obtuse, it follows that $0 \leq \angle C \leq \pi/4$, as well as $\angle C \leq \angle B \leq \pi/2 - \angle C/2$. Over this domain, it is easy to verify that $10\sin(2(B+C)) - 2\sin(4(B+C)) - \sin(4B+2C) + 2\sin(2B+4C) + 6\sin(2B) + 7\sin(2C) \geq 0$. Since also $(\cos(2(B+C)) - 2)^3 \leq 0$, it follows that $f(B, C)$ is decreasing in C , and hence

$$\begin{aligned}f(B, C) &\geq f(\pi/2 - C/2, C) \\ &= \frac{(-4\cos(2(\frac{C}{2} + \frac{\pi}{2})) - \cos(2(\frac{\pi}{2} - \frac{C}{2})) + 4\cos(2C) + 9)\sec^2(\frac{C}{2})}{2(\cos(2(\frac{C}{2} + \frac{\pi}{2})) - 2)^2} \\ &= \frac{8}{\cos(C) + 1} - \frac{27}{(\cos(C) + 2)^2}.\end{aligned}$$

The last function of C can be seen to be increasing in C , and when $C = 0$ it equals 1. This shows that $\|TB''\| / \|TG\| \geq 1$ as wanted.

Comparison to optimal RLD strategy: The proof of this case is more holistic. We determine the loci of points P that have the property that R_1 costs of the optimal RLD and optimal LRD visitations are equal. In its generality, the loci of points will be a mixed curve composed by a line segment, followed by a parabola segment, followed by a line segment. The mixed curve will split $\triangle ABC$ into regions in which one of the RLD or LRD strategy is strictly more efficient. As it will follow from the proof, the middle point of the shortest altitude of $\triangle ABC$, with $\angle A \geq \angle B \geq \angle C$, will either fall on that mixed curve, or on the side where the LRD strategy is strictly more efficient.

To compare the optimal LRD and RLD visitation costs, we consider reflection C' of C across AB , and reflection B' of B across $C'A$, see also Figure 24. We also consider reflection B'' of B across AC , and reflection C'' of C across $B''A$.

Moreover, consider the LRD and RLD bounce indicator lines, that are perpendicular to $C'B'$ and $C''B''$, respectively. Note that $C'B'$ and $C''B''$ (or their extensions) always intersect, say at point Q , unless they coincide (exactly when $\angle A = \pi/2$). Let also AH be the altitude of $\triangle ABC$ passing through A . The next observation will be useful in the following arguments.

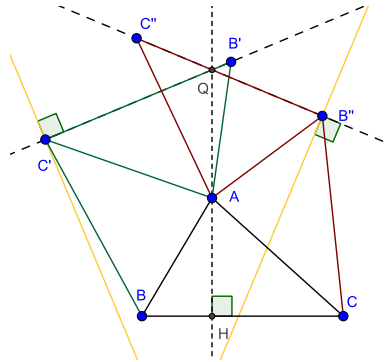


Fig. 24: The case of all points of altitude AH falling within the positive RLD and LRD bounce halfspaces.

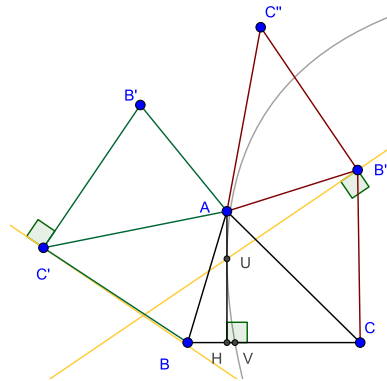


Fig. 25: The case of the positive RLD and negative LRD bounce halfspaces intersecting altitude AH .

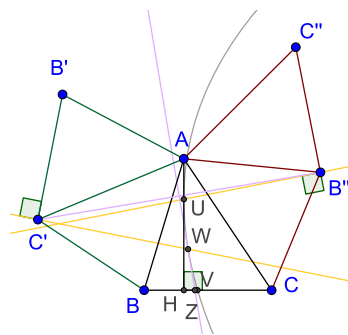


Fig. 26: The case of the negative RLD and LRD bounce halfspaces intersecting altitude AH .

Observation 7 *The extension ζ of the altitude AH passes also through the intersection Q of (the extensions of) $C'B'$ and $C''B''$. Moreover, unless $\angle A \neq \pi/2$, line ζ is also the bisector of one of the angles formed by (the extensions of) $C'B'$ and $C''B''$.*

Proof. Due to the already introduced reflections, the triangle formed by extensions of BC , $B'C'$ and $B''C''$ is isosceles. This means that QA is both the altitude and the bisector of angle Q of that isosceles triangle. Hence, it suffices to prove that QA is a bisector of the same angle Q . To that end, it is enough to show that A is equidistant from $B'C'$ and $B''C''$. The latter property is true since triangles $AB'C'$ and $AB''C''$ are equal, and hence have equal altitudes corresponding to A . \square

By Observation 7, all points P on the altitude AH are equidistant from the (extensions of) segments $B'C'$ and $B''C''$. Combined with the findings of Section 3.2, we conclude the following corollary.

Corollary 5. *If all points of altitude AH are in the positive bounce and subopt halfspaces of both LRD and RLD visitations, then the loci of points whose R_1 visitation cost is the same for the optimal LRD and RLD visitations is the altitude AH .*

If the indicator lines intersect in the interior of the altitude AH , then for any starting point in the negative halfspace of an indicator line, the optimal bouncing trajectory of the corresponding ordered visitation ends at a vertex. If $\angle A \geq \angle B \angle C$, the LRD indicator line intersects altitude AH at point U (closer to A than where the RLD indicator line might intersect AH), see also Figure 25.

For every starting point P in the intersection of the positive LRD bounce halfspace and the negative RLD bounce halfspace, the optimal LRD visitation is computed by $d(P, B'C')$ (and the projection of P onto $B'C'$ falls within $B'C'$). Also the optimal RLD visitation has cost $\|PB''\|$. Hence, the loci of points with same LRD and RLD costs is formed by all points that are equidistant from line $B'C'$ and point B'' . That would be the parabola with focus B'' and directrix $B'C'$.

Corollary 6. *The portion of loci of points with same LRD and RLD costs that lies within the intersection of the positive LRD and negative RLD bounce halfspaces is a (part of a) parabola with focus B'' and directrix $B'C'$.*

If the LRD indicator line intersects the aforementioned parabola outside $\triangle ABC$, then the loci of points with same LRD and RLD costs is formed by the portion of the altitude AU , followed by the portion of the parabola that lies within the given triangle (curve UV in Figure 25).

It remains to examine the case that the LRD bound indicator line intersects the parabola in the interior of triangle ABC , say at point W , see Figure 26. Then, for all starting points P in the intersection of the negative LRD and RLD bounce halfspaces, the optimal LRD and RLD visitations have cost $\|PC'\|$ and $\|PB''\|$, respectively. Hence, the loci of points with same LRD and RLD costs within these halfspaces are equidistant from points B'' and C' , hence they lie on the perpendicular bisector of segment $B''C'$, and let its intersection with line BC be Z .

Corollary 7. *The portion of loci of points with same LRD and RLD costs that lie within the intersection of the negative LRD and RLD bounce halfspaces is part of the perpendicular bisector of segment $B''C'$ that lies within triangle ABC .*

To conclude, in its generality (see Figure 26), the loci of points with same LRD and RLD costs is defined piecewise as, first a portion of altitude AH (segment AU), followed by a portion of parabola with focus B'' and directrix $B'C'$ (curve UW), followed by part of the perpendicular bisector of segment $B''C'$ (segment WZ). If in particular $\angle A \geq \angle B \geq \angle C$, and the middle of the shortest altitude is in the negative RLD bounce halfspace, it is immediate that the optimal LRD visitation is strictly more efficient than the optimal RLD visitation (and otherwise they are equal).

6 Visitation Trade-offs

6.1 Searching with 1 vs 3 Robots

Supremum Proof; 1 vs 3 Robots In this section we prove the following theorem.

Theorem 8. $\sup_{\Delta \in \mathcal{D}} \mathcal{R}_{1,3}(\Delta) = 4$.

The lower bound for $\sup_{\Delta \in \mathcal{D}} \mathcal{R}_{1,3}(\Delta)$ is given by the following simple lemma.

Lemma 14. *Let Δ be an equilateral triangle, and I be its incenter. Then, $R_1(I)/R_3(I) = 4$.*

Proof. The reader may consult Figure 12 for a depiction of the points. Let K be the projection of the incenter onto BC . By Lemma 10, an optimal trajectory for 1 robot would be to go to K , and then to A (following the bisector of A), inducing cost $R_1(I) = \|IK\| + \|KA\|$. At the same time, all angle bisectors in the equilateral triangle are also altitudes, so by Lemma 2, the cost for 3 robots equals $R_3(I) = \|IK\|$. The claim follows by noticing that, in equilateral triangles, $\|IK\| = \frac{1}{3} \|KA\|$. \square

The remaining of the section is devoted in proving a tight upper bound for

$$\sup_{\Delta \in \mathcal{D}} \mathcal{R}_{1,3}(\Delta).$$

In that direction, and for the remaining of the section, we consider a triangle $\Delta = ABC$ in standard analytic form. Without loss of generality, we also assume that the starting point P lies within the tetragon (4-gon) $AMIL$, see also Figure 6.

In order to provide the promised upper bound, we propose a heuristic upper bound for $R_1(P)$, as follows. Consider the projections P_1, P_2, P_3 of P onto AB, BC and CA respectively. Then, three (possibly) suboptimal visitation trajectories for one robot are $T_C(P) := \langle P, P_1, P, C, \rangle$, $T_A(P) := \langle P, P_2, P, A, \rangle$, $T_B(P) := \langle P, P_3, P, B, \rangle$, that is

$$R_1(P) \leq \min\{T_A(P), T_B(P), T_C(P)\}.$$
³

The proof of the upper bound follows directly by Lemma 15 and Lemma 17 below. At a high level, we further distinguish some of the heuristics $T_A(P), T_B(P), T_C(P)$, depending on $\angle A$.

³ Note we abuse notation and we denote by $T_A(P)$ both the trajectory and its cost.

Lemma 15. *If $\angle A \leq \pi/3$, then $\min\{T_B(P), T_C(P)\}/R_3(P) \leq 4$.*

Proof. Consider some starting point P in the tetragon $AMIL$ (see Figure 6). Let $\angle B', \angle C'$ denote angles $\angle CBP$ and $\angle PCB$, respectively, and note that since I is the incenter of the given triangle, then $\angle B' \geq \angle B/2$ and $\angle C' \geq \angle C/2$. At the same time, since P lies in tetragon $AMIL$ (and as a result of the partition of the given triangle using its bisectors) we have that $\max\{d(P, AB), d(P, AC)\} \leq d(P, BC)$, and in particular $R_3(P) = d(P, BC)$. But then,

$$\begin{aligned} \min \frac{\{T_B(P), T_C(P)\}}{R_3(P)} &= \frac{\min\{2d(P, AB) + \|PB\|, 2d(P, AC) + \|PC\|\}}{d(P, BC)} \\ &\leq 2 + \frac{\min\{\|PB\|, \|PC\|\}}{d(P, BC)} = 2 + \min\left\{\frac{1}{\sin(B')}, \frac{1}{\sin(C')}\right\}. \end{aligned}$$

Since $\angle A \leq \pi/3$, it follows that $\max\{\angle B, \angle C\} \geq \pi/3$. Therefore, $\max\{\angle B', \angle C'\} \geq \pi/6$, and moreover $\max\{\sin B', \sin C'\} \geq 1/2$, which implies the desired upper bound of 4. \square

Note that the proof of Lemma 15 provides evidence that $\min\{T_B(P), T_C(P)\}/R_3(P)$ is maximized when P is the incenter of the given triangle. The next lemma makes a similar observation for heuristic trajectory $T_A(P)$.

Lemma 16. *The ratio $T_A(P)/R_3(P)$ is maximized when P is either the incenter of Δ , or the intersections of the bisectors of B, C with AC, AB , respectively.*

Proof. Consider an arbitrary point P in the tetragon $AMIL$ (see Figure 6). We have that

$$\frac{T_A(P)}{R_3(P)} = \frac{2d(P, BC) + \|PA\|}{d(P, BC)} = 2 + \frac{\|PA\|}{d(P, BC)}.$$

Since Δ is non-obtuse, the closer P is to BC , the larger $\|PA\|$ is and the smaller $d(P, BC)$ is. In other words, $T_A(P)/R_3(P)$ attains its maximum for some point P in the line segments MI, IL . So, let us consider an arbitrary point P in the line segment IL . Clearly, it suffices to prove that $T_A(P)/R_3(P)$ is maximized either at I or at L . Equivalently, it suffices to prove that $\frac{\|PA\|}{d(P, BC)}$ is maximized either at I or at L .

First we show that $\angle LIA$ is strictly acute. Indeed, since Δ is non-obtuse, we have

$$\angle LIA = \pi - \angle A/2 - \angle ALI = \pi - \angle A/2 - (\pi - \angle B/2 - A) = (\angle A + \angle B)/2 < \pi/2.$$

This implies that the projection A_0 of A onto line passing through B, L , falls within the line segment IL . Now consider an arbitrary point

$$P_\lambda = (1 - \lambda)I + \lambda L$$

on the line segment IL , where $\lambda \in [0, 1]$. In particular, there exists $\lambda_0 \in (0, 1)$, such that $P_{\lambda_0} = A'$. Now, note that as λ increases from 0 to 1, it is immediate that $d(P_\lambda, BC)$ increases. Since $\angle LIA$ is non-obtuse, $\|P_\lambda A\|$ is decreasing when $\lambda \in [0, \lambda_0]$ and increasing when $\lambda \in [\lambda_0, 1]$. It follows that $\frac{\|P_\lambda A\|}{d(P_\lambda, BC)}$ attains its maximum either when $\lambda = 0$ or when $\lambda = 1$, that is, either at the incenter I or point L . \square

We are now ready to prove the lemma that complements Lemma 15.

Lemma 17. *If $\angle A \geq \pi/3$, then $T_A(P)/R_3(P) \leq 4$.*

Proof. By Lemma 16, it is enough to prove that $T_A(P)/R_3(P) \leq 4$, when P is either L or I , see also Figure 6. As before, we have

$$\frac{T_A(P)}{R_3(P)} = \frac{2d(P, BC) + \|PA\|}{d(P, BC)} = 2 + \frac{\|PA\|}{d(P, BC)},$$

therefore our goal is to show that $\frac{\|PA\|}{d(P, BC)} \leq 2$.

First, consider starting point $P = L$, and let L', L'' be the projections of L onto BC and AB , respectively. Note that $d(L, BC) = \|LL'\| = \|L'L''\| = R_3(L)$. In right $\triangle ALL''$ we have that $\sin(A) = \|LL''\| / \|AL\| = d(L, BC) / \|AL\|$. Since $\angle A \geq \pi/3$ we have $\sin(A) \geq 1/2$ and the claim follows.

Second, we focus on the starting point $P = I$, the incenter. For this we consider Δ in standard analytic form. Then,

$$\frac{T_A(I)}{R_3(I)} = \frac{2d(I, BC) + \|IA\|}{d(I, BC)} = 2 + \frac{\|IA\|}{d(I, BC)}.$$

Using Corollary 1 that gives the coordinates of incenter $I = (p_I, q_I)$ we can compute

$$\|IA\| = \sqrt{(p_I - p)^2 + (q_I - q)^2}, \quad d(I, BC) = q_I,$$

so that by Observation 1, we get, after some trigonometric manipulations, that

$$\frac{\|IA\|}{d(I, BC)} = \frac{1}{\cos\left(\frac{B+C}{2}\right)} \leq 2,$$

where the last inequality is due to that $\angle A \geq \pi/3$, and hence $\angle B + \angle C \leq 2\pi/3$. \square

Infimum Proof; 1 vs 3 Robots In this section we prove the following theorem.

Theorem 9. $\inf_{\Delta \in \mathcal{D}} \mathcal{R}_{1,3}(\Delta) = \sqrt{10}$.

The next lemma shows that $\inf_{\Delta \in \mathcal{D}} \mathcal{R}_{1,3}(\Delta) \leq \sqrt{10}$.

Lemma 18. *Let ABC be an isosceles with base BC . Then, we have*

$$\lim_{\angle A \rightarrow 0} \max_{P \in ABC} R_1(P)/R_3(P) = \sqrt{10}.$$

Proof. We consider a triangle in standard analytic form, with $B = (0, 0)$, $C = (1, 0)$ and $A = (1/2, q)$, with $q \rightarrow \infty$. For such a triangle, all the R_1 regions are summarized in Figure 14, and the optimal visitation strategies in Lemma 8. We need to show that for all starting points P , we have $R_1(P)/R_3(P) \leq \sqrt{10}$. By symmetry, we may restrict starting points in $\triangle ABK$, where K is the middle point of BC . We examine the following four regions of starting points: $BKH, DBH, DHJE$ and EJA .

First we analyze regions BKH, DBH together. Recall that E is identified by the optimal bouncing subcone of B , and that D is the projection of C onto AB . Note that as q grows, point D tends to B , and hence regions BKH, DBH tend to line segment BK . An arbitrary point in any of these regions (as $q \rightarrow \infty$), will tend to a point $P = (x, 0)$, where $0 \leq x \leq 1/2$. Clearly, $R_3(P) = 1 - x$. The optimal strategy in DBH is of LDR-type, and hence has cost (in the limit) $x + 1$. The optimal strategy in BKH is of DLR-type, and hence has cost (in the limit) $x + 1$. Overall, starting from P in any of the regions BKH, DBH , we have $R_1(P)/R_3(P)$ tends to $(x + 1)/(1 - x) \leq 3 < \sqrt{10}$.

Next we analyze region AEJ . The key observation is that a robot starting from that region can move parallel to BC (back and forth) visiting both AB, AC before moving to BC along the projection. Hence, $R_1(P) \leq 3/2 + R_3(P)$, or in other words, $R_1(P)/R_3(P) \leq 3/(2R_3(P)) + 1$. Next, we show that $R_3(P) \rightarrow \infty$ as $q \rightarrow \infty$ (i.e. as $\angle B \rightarrow \pi/2$), hence concluding this case as well. Indeed, any point in AEJ lies above the intersection of BF with AK , call it W . Since $\angle FBG = 3B - \pi$, it follows that $\angle FBC = \angle WBC = 2\angle B - \pi/2 \rightarrow \pi/2$, as $\angle B \rightarrow \pi/2$. Hence, W lies arbitrarily away from BC as $\angle B \rightarrow \pi/2$.

Finally, we analyze the region $EDHJ$. Starting from a point $P = (x, y)$, with $0 \leq x \leq 1/2$ and $0 \leq y \leq q$ (the latter bound is weak but does not affect our analysis), the optimal strategy for $R_1(P)$ is to bounce optimally to AB and then move to C . Equivalently, consider the reflection P' of P across AC . Then, as $q \rightarrow \infty$, we have $P' \rightarrow (x + 2(1 - x), y) = (2 - x, y)$, and therefore $R_1(P) \rightarrow \sqrt{(2 - x)^2 + y^2}$.

We consider three further subcases, and our underlying assumption remains that $0 \leq x \leq 1/2$ and $0 \leq y \leq q$. If P is (on or) above bisector of $\angle C$, then (in the limit) we have $y \geq -x + 1$ and $R_3(P) = y$. But then, we have

$$\frac{R_1(P)}{R_3(P)} \leq \sup_{y \geq -x+1} \frac{\sqrt{(2-x)^2 + y^2}}{y} = \sqrt{10},$$

achieved for $x, y \rightarrow 1/2$. If P is below the bisector of $\angle C$ and (on or) above the bisector of $\angle B$, then (in the limit) we have $x \leq y \leq -x + 1$, $y \geq x$, and $R_3(P) = 1 - x$. But then, we have

$$\frac{R_1(P)}{R_3(P)} \leq \sup_{x \leq y < -x+1} \frac{\sqrt{(2-x)^2 + y^2}}{1-x} = \sqrt{10},$$

achieved for $x, y \rightarrow 1/2$. Finally, if P is below bisector of $\angle B$, then (in the limit) we have $y \leq x$ and $R_3(P) = 1 - x$. But then, we have

$$\frac{R_1(P)}{R_3(P)} \leq \sup_{y < x} \frac{\sqrt{(2-x)^2 + y^2}}{1-x} = \sqrt{10},$$

achieved again for $x, y \rightarrow 1/2$. Note that worst starting point $P = (1/2, 1/2)$ is the (limit of the) incenter of thin isosceles ABC (as $\angle A \rightarrow 0$). \square

The next lemma shows that $\inf_{\Delta \in \mathcal{D}} \mathcal{R}_{1,3}(\Delta) \geq \sqrt{10}$.

Lemma 19. *For any triangle $\Delta \in \mathcal{D}$, let I denote its incenter. Then, we have $R_1(I)/R_3(I) \geq \sqrt{10}$.*

Proof. ⁴ Consider an arbitrary non-obtuse $\triangle ABC$ in standard analytic form. We assume that $\angle A$ is the largest angle. Let $I = (x, y)$ be its incenter, with coordinates given by Corollary 1. Since the incenter is equidistant from all triangle edges, and by Lemma 2, we have $R_3(I) = y$. Moreover, by Lemma 10, we have that

$$R_1(I) = \sqrt{(x-p)^2 + (y+q)^2}.$$

In what follows we prove the following claims:

Claim (a): $R_1(I)/R_3(I)$ is increasing in q , therefore it is minimized when $\angle A = \pi/2$.

Claim (b): The “thinner” a right triangle is, the smaller $R_1(I)/R_3(I)$ becomes.

Proof of Claim (a): Assume that $\angle A \leq \pi/2$ is the largest angle, and without loss of generality assume also that $p \in [0, 1/2]$. Note that

$$\frac{R_1(I)}{R_3(I)} = \frac{\sqrt{(x-p)^2 + (y+q)^2}}{y} = \sqrt{(x/y - p/y)^2 + (1+q/y)^2},$$

where in particular, $x = x(p, q)$ and $y = y(p, q)$. Since \sqrt{z} is an increasing function of z , it suffices to show that $(R_1(I)/R_3(I))^2$ is an increasing function of q . Note that the function we want to prove increasing in q is of the form $f^2(q) + g^2(q)$, where $f(q) = (x-p)/y \geq 0$ and $g(q) = 1 + q/y \geq 0$. Note that,

$$(f^2(q) + g^2(q))' = 2f(q)f'(q) + 2g(q)g'(q) \geq (f(q) + g(q))' \min\{f(q), g(q)\}.$$

Therefore, for $(R_1(I)/R_3(I))^2$ to be increasing in q , it suffices to prove that $f(q) + g(q) - 1 = (x-p)/y + q/y$ is increasing in q . To that end, we compute

$$\frac{\partial}{\partial q} ((x-p)/y + q/y) = \frac{h(p, q)}{\beta\gamma q^2},$$

where $h(p, q) := p^3(-(\beta+\gamma)) + p^2(\beta+2\gamma) - \gamma p + q^3(\beta+\gamma)$ and $\beta = \|AC\| = \sqrt{(1-p)^2 + q^2}$, $\gamma = \|AB\| = \sqrt{p^2 + q^2}$. Therefore, it further suffices to prove that $h(p, q) \geq 0$.

What we show next is that $h(p, q)$ preserves sign, condition on that $p, q > 0$, and on that $\angle A \leq \pi/2$. Indeed, we compute all roots of $h(p, q)$ with respect to q . Some tedious calculations show that $h(p, q)$ has two complex roots, and the real roots 0 and $q_{1,2} = \frac{-p^2 \pm \sqrt{-3p^4 + 6p^3 - 4p^2 + p + p}}{2p-1}$, among which only $q_1 = \frac{-p^2 - \sqrt{-3p^4 + 6p^3 - 4p^2 + p + p}}{2p-1}$ is non-negative for $p \in (0, 1/2]$. At the same time, $\angle A \leq \pi/2$, and hence $(p-1)^2 + q^2 \geq 1/4$. However, it is easy to show that

$$(p-1)^2 + q_1^2 \leq 1/4,$$

for all $p \in [0, 1/2]$, and equality holds only when $p = 0$. Therefore, continuous function $h(p, q)$ has no real roots in the domain $p, q > 0$ and $(p-1)^2 + q^2 \geq 1/4$, and hence must preserve sign. The sign is the same as the sign of $h(1/2, 1) = \sqrt{5} > 0$, as wanted.

⁴ The provided proof uses algebraic tools of analytic geometry. An alternative approach, using Observation 1, is to show, using trigonometric manipulations, that $(R_1(I)/R_3(I))^2 = \frac{4\cos(B)+4\cos(C)+2}{\cos(A)+1} + 4$. Then, one would need to minimize the latter expression over the domain of non-obtuse triangles $\triangle ABC$ with dominant angle A .

Proof of Claim (b): Consider arbitrary right triangle $A = (p, q), B = (0, 0), C = (1, 0)$, with $\angle A = \pi/2$. Point A must lie on a cycle with radius $1/2$ and center $(1/2, 0)$, and hence $(p - 1/2)^2 + q^2 = 1/2^2$, from which we conclude that $q = \sqrt{p - p^2}$. Using Corollary 1 we obtain that

$$I = \left(\frac{1}{2} \left(-\sqrt{1-p} + \sqrt{p} + 1 \right), \frac{\sqrt{(1-p)p}}{\sqrt{1-p} + \sqrt{p} + 1} \right).$$

Then, using the discussion above, and after elementary calculations, we see that

$$\frac{R_1(I)}{R_3(I)} = \sqrt{4\sqrt{1-p} + 4\sqrt{p} + 6}.$$

It is easy to see that $4\sqrt{1-p} + 4\sqrt{p} + 6$ preserves positive sign, and it is increasing p . Therefore, its square is increasing, that is $R_1(I)/R_3(I)$ is increasing in p .

To conclude, using claims (a),(b) above, we have

$$\inf \frac{R_1(I)}{R_3(I)} \geq \lim_{p \rightarrow 0} \sqrt{4\sqrt{1-p} + 4\sqrt{p} + 6} = \sqrt{10},$$

and the proof is finished. \square

6.2 Searching with 2 vs 3 Robots

Supremum Proof; 2 vs 3 Robots In this section we prove the following theorem.

Theorem 10. $\sup_{\Delta \in \mathcal{D}} \mathcal{R}_{2,3}(\Delta) = 2$.

The next lemma shows that $\sup_{\Delta \in \mathcal{D}} \mathcal{R}_{2,3}(\Delta) \geq 2$.

Lemma 20. *Let ABC be an equilateral triangle with incenter I . Then, we have $R_2(I)/R_3(I) = 2$.*

Proof. The incenter I is equidistant from all edges AB, BC, CA , and hence by Lemma 2, we have $R_3(I) = d(I, BC)$. Also, by Lemma 9, we have $R_2(I) = \|IA\|$, and therefore

$$\frac{R_2(I)}{R_3(I)} = \frac{\|IA\|}{d(I, BC)}.$$

Now recall that $\triangle ABC$ is equilateral, therefore each of the bisectors coincide with the altitudes. Moreover, I is the center of the regular triangle, and hence its apothem (with length $d(I, BC)$) is $1/3$ of the altitude. The main claim follows by noting that $\|IA\|$ makes up the remaining $2/3$ of the altitude. \square

The remaining of the section is devoted in proving that $\sup_{\Delta \in \mathcal{D}} \mathcal{R}_{2,3}(\Delta) \leq 2$. In that direction, we consider a triangle $\Delta = ABC$ along with its incenter I , see also Figure 6. Without loss of generality, we also assume that the starting point P lies within the $\triangle AIL$,

In order to provide the promised upper bound, we propose a heuristic upper bound for $R_2(P)$. The two robots visit all edges as follows; one robot goes to the vertex corresponding to the largest angle (visiting the two incident edges), and the second robot visits the remaining edge moving along the projection of P along that edge. Note that the largest angle is at least $\pi/3$.

Lemma 21. *If the largest angle is $\angle A$, then $R_2(P)/R_3(P) \leq 2$.*

Proof. Consider an arbitrary point P in $\triangle AIL$. Due to the heuristic strategy of $R_2(P)$, one robot goes to A in time $\|PA\|$, and the other robot goes to edge BC in time $d(P, BC)$. So overall, we have

$$R_2(P) \leq \max\{\|PA\|, d(P, BC)\}.$$

Since $R_3(P) = d(P, BC)$, it follows that if $\|PA\| < d(P, BC)$, then $R_2(P)/R_3(P) = 1$. On the other hand, if $\|PA\| \geq d(P, BC)$, then we have

$$\frac{R_2(P)}{R_3(P)} \leq \frac{\|PA\|}{d(P, BC)}. \quad (10)$$

Recall that P lies in $\triangle AIL$. By the proof of Lemma 16, ratio (10) is maximized either at the incenter, or at point L . Then, by the proof of Lemma 17, and since $\angle A \geq \pi/3$ the same ratio is at most 2. \square

Lemma 22. *If the largest angle is either $\angle B$ or $\angle C$, then $R_2(P)/R_3(P) \leq 2$.*

Proof. We provide the proof of the case that $\angle C$ is the largest angle, and hence at least $\pi/3$ (the other case is identical). For every point P in $\triangle AIL$, we have that $R_3(P) = d(P, BC)$ (see Section 4.1). Due to the heuristic we are using, the claim follows once we show that $\frac{\max\{\|PC\|, d(P, AB)\}}{d(P, BC)} \leq 2$. Note that $d(P, AB) \leq d(P, BC)$, and so, if

$$\max\{\|PC\|, d(P, AB)\} = d(P, AB),$$

it follows that $R_2(P)/R_3(P) \leq 1$.

It remains to examine the case $R_2(P) = \|PC\|$. To that end, note that $\angle PCB \geq \angle C/2 \geq \pi/6$. Since moreover the sin function is increasing in $[0, \pi/2]$, we have

$$\frac{\|PC\|}{d(P, BC)} = \frac{1}{\sin(\angle PCB)} \leq \frac{1}{\sin(\pi/6)} = 2$$

as wanted. \square

Infimum Proof; 2 vs 3 Robots In this section we prove the following theorem.

Theorem 11. $\inf_{\Delta \in \mathcal{D}} \mathcal{R}_{2,3}(\Delta) = \sqrt{2}$.

The next lemma shows that $\inf_{\Delta \in \mathcal{D}} \mathcal{R}_{2,3}(\Delta) \leq \sqrt{2}$

Lemma 23. *Let $\triangle ABC$ be a right isosceles with $\angle A = \pi/2$. Then, we have*

$$\max_{P \in ABC} R_2(P)/R_3(P) = \sqrt{2}.$$

Proof. Consider right isosceles $\triangle ABC$ with $\angle A = \pi/2$. For such a triangle, The R_3 regions are summarized in Lemma 2. Also, all R_2 regions are summarized in Corollary 3 and Lemma 5, see also Figure 11.

We conclude that the R_2 regions of right isosceles ABC with $\angle A = \pi/2$ are determined by the refined R_2 separator $MFJKLQ$ and the incenter I . More specifically, for every starting point P outside $MFJKLQ$, cost $R_2(P)$ is determined by the cost of visiting the more distant edge (and hence it equals $R_3(P)$). Hence,

$$\arg \max_{P \in ABC} R_2(P)/R_3(P)$$

lies within $MFJKLQ$, and by symmetry, we may further assume that P lies in $MFAQ$.

We consider the analytic representation of right isosceles ABC , that is we set $A = (1/2, 1/2), B = (0, 0), C = (1, 0)$. Using Corollary 1, the incenter is $I = (1/2, 1/\sqrt{2} - 1/2)$. By Lemma 9, we have that $R_2(I) = \|IA\| = 1 - 1/\sqrt{2}$. Recalling also that $R_3(I) = d(I, BC) = 1/\sqrt{2} - 1/2$, it follows that $R_2(I)/R_3(I) = \sqrt{2}$. Below, we show that

$$\arg \max_{P \in MFAQ} R_2(P)/R_3(P) \leq \sqrt{2}.$$

In what follows, we commonly denote $P = (a, b)$, for any placement of P . Combined with the partition of ABC that determines all costs $R_3(P)$, as per Section 4.1, we are motivated to consider the following four cases.

Case 1, $P \in MIQ$: We have that $R_2(P) = \|PA\|$ and $R_3(P) = d(P, BC)$. Clearly, $R_2(P)$ is maximized either at $P = M$ or at $P = I$ (one of which may be a local maximizer). Note that $\angle AMC = \pi - \angle A - \angle MCA = \pi - \angle A - \angle C/2 = \pi - \pi/2 - \pi/8 = 3\pi/8$. Since $\angle MAI = \pi/4$, it follows that $\triangle AMI$ is isosceles, and therefore $\|MA\| = \|IM\|$. We conclude that $R_2(P)$ is maximized at $P = I$. At the same time, $R_3(P)$ is clearly minimized at $P = I$. Hence, $\arg \max_{P \in MFAQ} R_2(P)/R_3(P) = I$.

Case 2, $P \in MTUI$: We have that $R_2(P) = \|PA\| = \sqrt{(a - \frac{1}{2})^2 + (b - \frac{1}{2})^2}$. Also, the line passing through A, C has equation $x + y - 1 = 0$, hence $R_3(P) = d(P, AC) = |a + b - 1|/\sqrt{2}$. Let $f(a, b) = (R_2(P)/R_3(P))^2$, and note that

$$\nabla f(a, b) = 2 \frac{a - b}{(a + b - 1)^3} \begin{pmatrix} 2b - 1 \\ -2a + 1 \end{pmatrix}.$$

Observe that $a < b$, and that $a + b - 1 < 1$, hence directions $e_1, -e_2$ are both increasing. It follows that when $P \in MTUI$, ratio $R_2(P)/R_3(P)$ is maximized at $P = U$. At the same time, point U lies on line $x = 1/2$, and easy calculations show that $f(1/2, b) = 2$ (that is, the function is constant), concluding this case as well.

Case 3, $P \in MFT$: As before, we have $R_3(P) = d(P, AC) = |a + b - 1|/\sqrt{2}$. The optimal strategy for $R_2(P)$ is of LD-type. Let P' be the reflection of P around AB , that is $P' = (b, a)$. It follows that $R_2(P) = d(P', BC) = a$, and therefore $(R_2(P)/R_3(P))^2 = 2a^2/(a + b - 1)^2$. It is easy to see that the last ratio is at most 2, exactly when $(b - 1)(2a + b - 1) \geq 0$. Note also that $b \leq 1/2 < 1$, hence it suffices to prove that $2a + b - 1 \leq 0$ for all $P \in MFT$.

In region MFT , curve MT is part of a parabola with directrix $x = 0$ and focus $A = (1/2, 1/2)$, hence it has equation $(y - 1/2)^2 = x - 1/4$. It follows that point $P = (a, b)$ satisfies $(b - 1/2)^2 \geq a - 1/4$. Since also P is on or below line segment AB (with line equation $y = x$), it follows $a \geq b$, whereas we also have $a \geq 0$. So we consider the following non-linear program

$$\max\{2a + b - 1 : b \leq a \leq (b - 1/2)^2 + 1/4, a \geq 0\},$$

and we show that its value is bounded above by 0. Note the the objective is linear, so the gradient is never the zero-vector. Therefore any optimizers are attained by making some of the inequality constraints tight.

If $a \leq 0$ becomes tight, then $2a + b - 1 = b - 1 \leq -1/2$. If $b \leq a$ becomes tight, then $P = M$, and that point was already considered in cases 1,2. It remains to examine the case that constraint $a \leq (b - 1/2)^2 + 1/4$ is tight, that is when P lies in the curve segment MT which is contained in region $MTUI$ already considered in case 2.

Case 4, $P \in FKUT$: Again, we have $R_3(P) = d(P, AC) = |a + b - 1| / \sqrt{2}$. The optimal strategy for $R_2(P)$ is now of DL-type. Let P'' be the reflection of P around BC , that is $P'' = (a, -b)$. It follows that $R_2(P) = d(P'', AC) = |a + b| / \sqrt{2}$. Taking into consideration that $a, b \geq 0$, and that $a + b \leq 1$ (for any point $P = (a, b)$, within ABC), we have that $g(a, b) := (R_2(P)/R_3(P))^2 = (a + b)/(1 - a - b)$, which we show next is at most $\sqrt{2}$.

Curve TU of region $FKUT$ is part of a parabola with directrix the reflection of AB around BC (that is line $y = -x$), and focus $A = (1/2, 1/2)$. Therefore the equation of the parabola is $(x - 1/2)^2 + (y - 1/2)^2 = (x + y)^2 / 2$. We conclude that points $P \in FKUT$ satisfy $(a - 1/2)^2 + (b - 1/2)^2 \geq (a + b)^2 / 2$. At the same time we have that $x \leq 1/2$, so it suffices to prove that optimal value to non-linear program $\max\{g(a, b) : (a - 1/2)^2 + (b - 1/2)^2 \geq (a + b)^2 / 2, a \leq 1/2\}$ is at most $\sqrt{2}$.

To that end, we observe that $\partial g(a, b) / \partial a = 1 / (1 - a - b)^2 \geq 0$, that is e_1 is an increasing direction. We conclude that optimizers of the previous optimization problem within $FKUT$ happen either at line segment UK , or at curve segment TU .

As curve segment TU is contained within region $MTUI$ (already considered in case 2), it remains to examine the case that P lies in line segment UK , that is $a = 1/2$. But then, $g(1/2, b) = 1 / (1/2 - y) - 1$, which is further maximized when y attains its maximum value, i.e. when P coincides with point U , and that point was also considered in case 2.

□

The next lemma shows that $\inf_{\Delta \in \mathcal{D}} \mathcal{R}_{2,3}(\Delta) \geq \sqrt{2}$.

Lemma 24. *For any triangle $\Delta \in \mathcal{D}$, let I denote its incenter. Then, we have $R_2(I) / R_3(I) \geq \sqrt{2}$.*

Proof. Consider $\triangle ABC$ with largest angle C , and incenter I . Since I is equidistant from all edges, and by Lemma 2, we have $R_3(I) = d(I, BC)$. Moreover, since $C \geq \pi/3$, by Lemma 9, we have that $R_2(I) = \|IC\|$. But then, since $\triangle ABC$ is non-obtuse, we have $C \leq \pi/2$, and so

$$\frac{R_2(I)}{R_3(I)} = \frac{\|IC\|}{d(I, BC)} = \frac{1}{\sin(C/2)} \geq \frac{1}{\sin(\pi/4)} = \sqrt{2}.$$

This finishes the proof of the lemma.

□

6.3 Searching with 1 vs 2 Robots

Supremum Proof; 1 vs 2 Robots In this section we prove the following theorem.

Theorem 12. $\sup_{\Delta \in \mathcal{D}} \mathcal{R}_{1,2}(\Delta) = 3$.

As we show next, the lower bound for $\sup_{\Delta \in \mathcal{D}} \mathcal{R}_{1,2}(\Delta)$ is attained for the right isosceles triangle (and for certain starting point). The upper bound is much easier and is presented next.

Lemma 25. *For any non-obtuse triangle $\Delta \in \mathcal{D}$, and any starting point $P \in \Delta$, we have $R_1(P)/R_2(P) \leq 3$.*

Proof. Consider a non-obtuse $\triangle ABC$, and a point P . Without loss of generality, assume that $R_2(P) = \max\{d(P, AB), d(P, \{BC, CA\})\}$. Note that for the $R_2(P)$ solution, one robot follows the optimal trajectory for visiting AB and the other follows the optimal trajectory for visiting $\{BC, CA\}$. Let T_c be the least expensive of the two trajectories, and T_e be the most expensive (and break ties arbitrarily if their costs are equal).

It suffices to present a heuristic trajectory that one robot could follow that does not cost more than $3R_2(P)$. Indeed, starting from P , first move along the cheapest trajectory T_c and return to point P , followed by moving along T_e . Clearly, this trajectory visits all $\{AB, BC, CA\}$, and takes time

$$2 \min\{d(P, AB), d(P, \{BC, CA\})\} + \max\{d(P, AB), d(P, \{BC, CA\})\},$$

which is at most $3 \max\{d(P, AB), d(P, \{BC, CA\})\} = 3R_2(P)$. Since the optimal $R_1(P)$ has cost at most the cost of the heuristic solution, it follows that $R_1(P)/R_2(P) \leq 3$. \square

In order to prove a matching upper bound, we present a non-obtuse triangle and a starting point for which the optimal R_1 trajectory is exactly the heuristic used in the proof of Lemma 25. Indeed, the next lemma shows that $\sup_{\Delta \in \mathcal{D}} \mathcal{R}_{1,2}(\Delta) \geq 3$, and together with the previous lemma imply Theorem 12.

Lemma 26. *Let ABC be a right isosceles triangle with right angle A . Let also P be the middle point of the altitude corresponding to angle A . Then, $R_1(P)/R_2(P) = 3$.*

Proof. Note that $\angle A \geq \pi/3$, so starting point P lies in the intersection of angle A bisector and the corresponding separating parabola. In particular $R_2(P) = d(P, BC) = d(P, \{AB, AC\}) = \|AP\|$. Without loss of generality, we may assume that $\|BC\| = 1$, and hence $\|AB\| = \|AC\| = \sqrt{2}/2$, so that $R_2(P) = 1/4$. Note also that by Lemma 13, the optimal R_1 strategy is of LRD type. More specifically, using $\angle A = \pi/2, \angle B = \angle C = \pi/4$ and substituting in cost function gives $R_1(P) = 3/4$, and the claim follows. \square

Infimum Proof; 1 vs 2 Robots In this section we prove the following theorem.

Theorem 13. $\inf_{\Delta \in \mathcal{D}} \mathcal{R}_{1,2}(\Delta) = 5/2$.

The next lemma shows that $\inf_{\Delta \in \mathcal{D}} \mathcal{R}_{1,2}(\Delta) \leq 5/2$.

Lemma 27. *Consider an equilateral triangle Δ . Then, we have $\max_{P \in \Delta} R_1(P)/R_2(P) = 5/2$.*

Proof. We consider equilateral $\triangle ABC$, with bisectors (and altitudes) AK, BL, CM , and incenter I , see also Figure 27. Let also W be the intersection of ML with AK . By symmetry, it is enough to show that $\max_{P \in AMI} R_1(P)/R_2(P) = 5/2$. Below we use the R_1 regions that are summarized in Lemma 6, and the R_2 regions, that are summarized in Corollary 2 and Corollary 4.

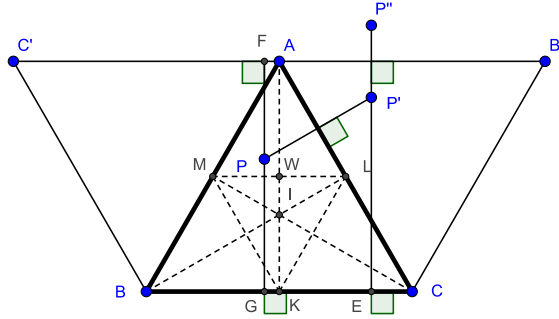


Fig. 27: Equilateral $\triangle ABC$, and comparison of optimal R_1, R_2 strategies for arbitrary starting points.

In particular, R_1 and R_2 regions are determined by the bisectors and points K, L, M . More specifically, consider the reflections C', P', B', P'' of C, P, B, P' around AB, AC, AC, AB' , respectively. We also assume that the triangle is in standard analytic form, i.e. we set $A = (p, q)^T, B = (0, 0)^T, C = (1, 0)^T$ in a Cartesian system (here we treat points as column vectors so as to perform some linear algebra manipulation), where $p = 1/2$ and $q = \sqrt{3}/2$.

For every $P \in AMI$, the optimal R_1 strategy is LRD-type, and hence $R_1(P) = d(P'', BC)$. Note also that P'' is obtained by rotating P by $2\pi/3$ with center A . Hence, if $P = (a, b)^T$ we have that

$$P'' = R_{2\pi/3}(P - A) + A = R_{2\pi/3} \left(\begin{pmatrix} a \\ b \end{pmatrix} - \begin{pmatrix} p \\ q \end{pmatrix} \right) + \begin{pmatrix} p \\ q \end{pmatrix}.$$

Since also $d(P'', BC)$ equals the second coordinate of P'' , we have that

$$R_1(P) = \sin(2\pi/3)(a - p) + (\cos(2\pi/3)(b - q) + q) = \frac{\sqrt{3}}{2}(a - p) - \frac{1}{2}(b - q) + q.$$

For starting points $P \in AMI$, we have two cases regarding the cost of the optimal R_2 strategy. If $P \in AMW$, then we have $R_2(P) = \|PG\| = b$. If $P \in MIW$, then the dominant cost for the R_2 strategy is due to a robot that visits AB, AC . Note also that $d(P, \{AB, AC\}) = d(P, AC') = q - b$. Overall, we have that for all $P \in AMI$

$$R_2(P) = \max\{b, q - b\}.$$

Combining the above, we have that

$$\begin{aligned} \max_{P \in AMI} \frac{R_1(P)}{R_2(P)} &= \max_{a,b} \frac{\frac{\sqrt{3}}{2}(a - 1/2) - \frac{1}{2}(b - \sqrt{3}/2) + \sqrt{3}/2}{\max\{b, \sqrt{3}/2 - b\}} \\ &\stackrel{(a \leq 1/2)}{\leq} \max_b \frac{-\frac{1}{2}(b - \sqrt{3}/2) + \sqrt{3}/2}{\max\{b, \sqrt{3}/2 - b\}} \\ &= \frac{5}{2}, \end{aligned}$$

i.e. the maximum is attained at $a = 1/2, b = \sqrt{3}/4$ which is point W . \square

The next lemma shows that $\inf_{\Delta \in \mathcal{D}} \mathcal{R}_{1,2}(\Delta) \geq 5/2$.

Lemma 28. *For any $\Delta ABC \in \mathcal{D}$, let T be the middle point of the altitude corresponding to the largest edge. Then, we have $R_1(T)/R_2(T) \geq 5/2$.*

Proof. Without loss of generality, we assume that BC is the largest edge of non-obtuse ΔABC , hence $\angle A$ is the largest angle. Consider the standard analytic representation of ABC . By Lemma 4, we have that $R_2(T) = d(T, BC) = q/2$, which can be expressed by Observation 1 using only triangle angles. By Lemma 13, we also have that the optimal strategy of $R_1(T)$ is of LRD type and the cost is expressed as a function of the angles. But then, it is immediate that $R_1(T)/R_2(T) = 2 - \cos(2A) \geq 5/2$, where the last inequality is due to that $\angle A \geq \pi/3$. \square

7 Conclusions

We considered a new vehicle routing-type problem in which (fleets of) robots visit all edges of a triangle. We proved tight bounds regarding visitation trade-offs with respect to the size of the available fleet. In order to avoid degenerate cases of visiting the edges with 3 robots, we only focused our study on non-obtuse triangles. The case of arbitrary triangles, as well as of other topologies, e.g. graphs, remains open. We believe the definition of our problem is of independent interest, and that the study of efficiency trade-offs in combinatorial problems with respect to the number of available processors (that may not be constant as in our case), e.g. vehicle routing type problems, will lead to new, deep and interesting questions.

References

1. Sumi Acharjee, Konstantinos Georgiou, Somnath Kundu, and Akshaya Srinivasan. Lower bounds for shoreline searching with 2 or more robots. In Pascal Felber, Roy Friedman, Seth Gilbert, and Avery Miller, editors, *23rd International Conference on Principles of Distributed Systems (OPODIS'19)*, volume 153 of *LIPIcs*, pages 26:1–26:11. Schloss Dagstuhl - Leibniz-Zentrum für Informatik, 2019.
2. Sanjeev Arora. Polynomial time approximation schemes for Euclidean traveling salesman and other geometric problems. *J. ACM*, 45(5):753–782, 1998.

3. Ricardo Baeza-Yates and René Schott. Parallel searching in the plane. *Computational Geometry*, 5(3):143–154, 1995.
4. Ricardo A Baeza-Yates, Joseph C Culberson, and Gregory JE Rawlins. Searching with uncertainty. In *Scandinavian Workshop on Algorithm Theory*, pages 176–189. Springer, 1988.
5. Tolga Bektas. The multiple traveling salesman problem: an overview of formulations and solution procedures. *Omega*, 34(3):209–219, 2006.
6. George B Dantzig and John H Ramser. The truck dispatching problem. *Management science*, 6(1):80–91, 1959.
7. Aparna Das and Claire Mathieu. A quasipolynomial time approximation scheme for Euclidean capacitated vehicle routing. *Algorithmica*, 73(1):115–142, 2015.
8. Stefan Dobrev, Rastislav Kráľovič, and Dana Pardubská. Improved lower bounds for shoreline search. In *Structural Information and Communication Complexity - 27th International Colloquium, SIROCCO 2020, Paderborn, Germany*, Lecture Notes in Computer Science. Springer, 2020.
9. Adrian Dumitrescu and Csaba D. Tóth. The traveling salesman problem for lines, balls, and planes. *ACM Trans. Algorithms*, 12(3):43:1–43:29, 2016.
10. Suresh Nanda Kumar and Ramasamy Panneerselvam. A survey on the vehicle routing problem and its variants. *Intelligent Information Management*, 4(3):66–74, 2012.
11. G. Laporte. The vehicle routing problem: An overview of exact and approximate algorithms. *European Journal of Operational Research*, 59:345–358, 1992.
12. Andrea Mor and Maria Grazia Speranza. Vehicle routing problems over time: a survey. *4OR*, pages 1–21, 2020.
13. Ulrike Ritzinger, Jakob Puchinger, and Richard F Hartl. A survey on dynamic and stochastic vehicle routing problems. *International Journal of Production Research*, 54(1):215–231, 2016.
14. P. Tóth and D. Vigo. The vehicle routing problem. monographs. *Discrete Mathematics and Applications, Society for Industrial and Applied Mathematics, Philadelphia*, 2002.